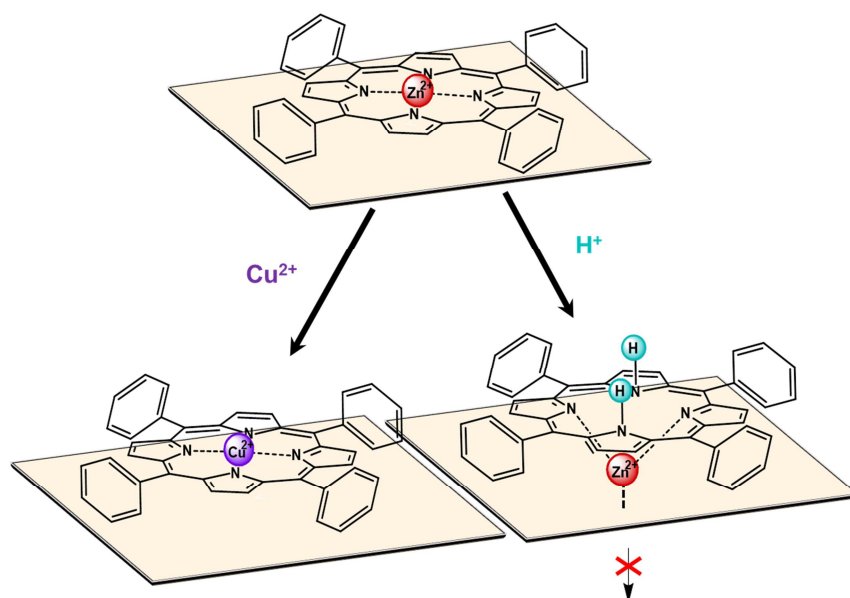


Porphyrin Reactions on Oxide Surfaces and in the Liquid Phase & Anhydride Formation on a Silver Surface

Porphyrin Reaktionen an Oxidoberflächen und in flüssiger Phase
&
Anhydridbildung auf einer Silberoberfläche



Der Naturwissenschaftlichen Fakultät der Friedrich-Alexander-Universität
Erlangen-Nürnberg
zur Erlangung des Doktorgrades Dr. rer. nat.

vorgelegt von
Matthias Franke
Aus Chemnitz

Als Dissertation genehmigt
von der Naturwissenschaftlichen Fakultät
der Friedrich-Alexander-Universität Erlangen-Nürnberg
Tag der mündlichen Prüfung: 14.03.2017

Vorsitzender des Prüfungsorgans: Prof. Dr. Georg Kreimer

Gutachter/in: Prof. Dr. Hans-Peter Steinrück
Prof. Dr. Federico José Williams

Content

1	Introduction.....	2
1.1	Porphyrin adsorption on surfaces.....	3
1.2	Porphyrin metalation: homogeneous liquids vs metal surfaces	5
2	Experimental methods.....	6
2.1	X-Ray Photoelectron Spectroscopy (XPS)	6
2.1.1	XPS basics	6
2.1.2	The XP spectrum.....	7
2.1.3	Core level shifts	8
2.1.4	Coverage determination with XPS.....	9
2.2	Ultra-Violet Photoelectron Spectroscopy (UPS)	11
2.3	Temperature-Programmed Desorption (TPD)	12
3	Experimental details.....	14
3.1	Setup	14
3.2	Sample preparation	15
3.2.1	MgO thin film growth.....	15
3.2.2	Liquid phase experiments	17
3.3	Water purification	18
4	Results.....	20
4.1	Porphyrins at solid/liquid interfaces	20
4.2	Porphyrin adsorption and reactions on MgO thin films.....	26
4.3	Anhydride formation on a silver surface.....	30
5	Conclusion	36
6	Outlook	38
7	Zusammenfassung.....	39
8	Acknowledgement	41
9	List of References	42
10	Appendix [P1]-[P5]	48

1 Introduction

When it comes to the development of functional devices, scientists and engineers have often been inspired by biology. Evolution has spent millions of years optimizing processes in living beings so they can survive in their environment. Photosynthesis, metabolism and nerve conduction are just a few examples. These three examples have one similarity: a class of molecules called porphyrins plays a vital role in all of them.¹ Porphyrins are planar organic molecules and consist of four pyrrole rings (C_4H_4N), linked together by methine ($=CH-$) bridges. The four nitrogen atoms in the center of the molecule form a central cavity which can either coordinate two protons (free-base porphyrin) or a metal center (metalloporphyrin). A few examples of biologically important porphyrin derivatives are

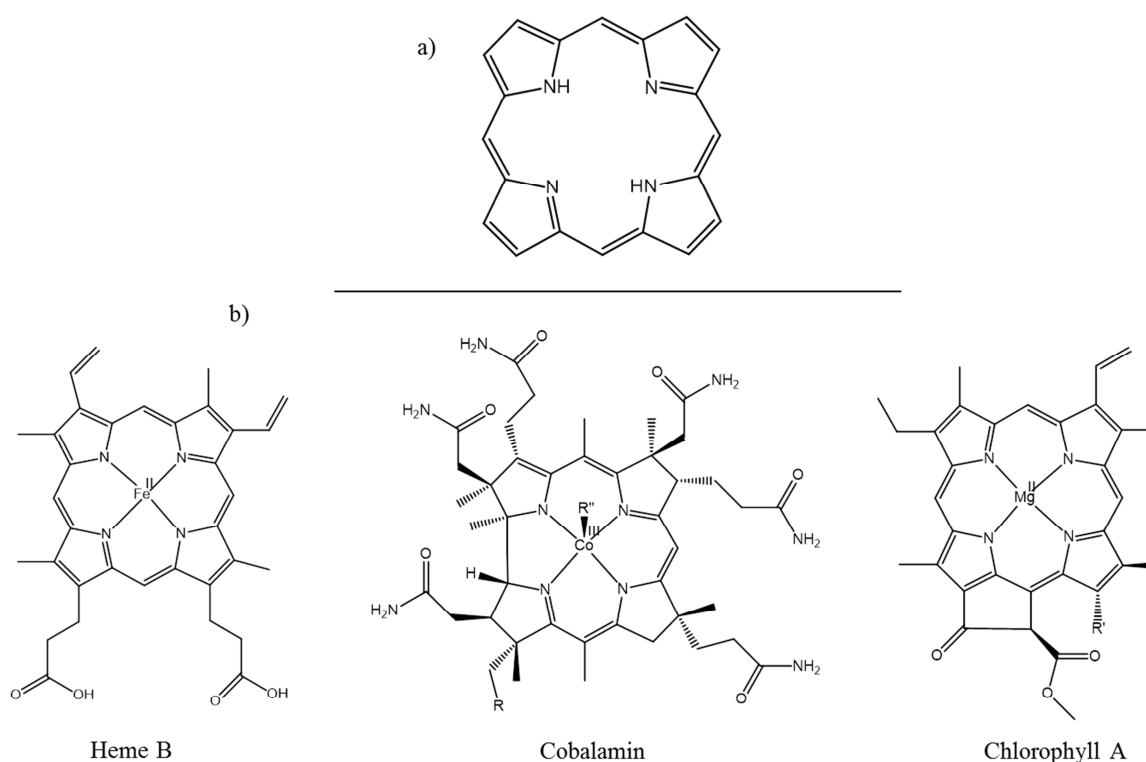


Figure 1. a) Porphine, the basic porphyrin unit, b) examples for functional porphyrins in nature

Chlorophyll A, Heme B and Cobalamin.^{2,3,4} Chlorophyll A, a magnesium(II)-porphyrin, is responsible for light harvesting and electron transfer in the photosynthesis of green plants. Upon light adsorption, an excited state is formed which is a strong reduction agent and provides electrons that are finally used for the reduction of CO_2 , after being transferred along a chain of different acceptors.⁵ Heme B, an iron(II)-porphyrin, is a part of the proteins hemoglobin and myoglobin which are responsible for transport and storage of oxygen in mammalian blood cells. Cobalamin, or Vitamin B12, plays a key role for the function of the nervous systems and the formation of red blood cells; it consists of a cobalt(III)-porphyrin.

The examples show that porphyrins can fulfill a variety of different tasks depending on the metal center bound to the central cavity and the side groups attached to the macrocycle. Due to their versatility and often high stability, they have not only attracted fundamental research interest,⁶ but are also highly interesting for technical applications. Indeed, porphyrins have been shown to be promising candidates for, for instance, dye-sensitized solar cells.^{7,8} In TiO₂-based dye-sensitized solar cells, porphyrins fulfill a similar task as in the photosynthesis acting as light absorber and part of the redox system. It has been shown that the performance of the solar cell depends on the type of bond between porphyrins and the oxide.⁷ Other potential applications include colorimetric gas sensing⁹ and catalysis.¹⁰

As lots of those applications rely on thin porphyrin films on a solid support, the interaction between porphyrins and solid surfaces has gathered significant research interest in the past decades.^{11,12,13} Most of the research work has so far been conducted on metal single-crystal surfaces in vacuum and the knowledge about fundamental interactions and principles is consequently also limited to these well-defined systems. However, adsorption on oxide surfaces and exposure to liquids have to be considered for many porphyrin-based devices, for instance in the above-mentioned dye-sensitized solar cells, where the dyes are adsorbed on a wide-band gap semiconductor and in contact with an electrolyte solution.⁸

The aim of the present thesis is to fill this knowledge gap by improving the understanding of porphyrin/oxide and porphyrin/liquid interfaces. Since controlling metal center coordination is crucial for tailoring the functionality of porphyrins, a major focus of this work will be the synthesis of metalloporphyrins from free-base molecules (metalation reaction) and other metalloporphyrins (metal center exchange) at the mentioned interfaces.

This dissertation is a cumulative thesis, which is based on five publications with exclusive or major contributions from the author (four have already appeared and one is close to submission). The work was performed in collaboration with the groups of Prof. Federico Williams (Universidad de Buenos Aires), Prof. Oliver Diwald (Universität Salzburg) and Prof. Bernd Meyer in Erlangen. In the next chapters, an introduction in the scientific topic (Chapters 1.1 and 1.2), an overview of the applied techniques and the setups (Chapter 2), and of the experimental details (Chapter 3) is given, followed by an extended summary of the achieved results (Chapter 4).

1.1 Porphyrin adsorption on surfaces

In the following paragraph, available literature on porphyrin surface science is summarized only briefly. For a more detailed examination, the reader is referred to recently published review articles.^{11,12}

The energy gain during porphyrin adsorption on a metal surface is mainly due to van-der-Waals forces. Consequently, this interaction is maximized and the molecules usually adsorb with their

macrocycle aligned parallel to the surface.¹⁴ However, some porphyrin derivatives are not planar because their peripheral substituents are not able to align coplanar with the flat macrocycle for steric reasons. Tetraphenylporphyrin (TPP), which was used for the experiments in this thesis, belongs to the group of non-planar porphyrins. The rotation of the TPPs phenyl rings is sterically hindered by the macrocycle; therefore the equilibrium gas phase conformation exhibits phenyl legs, which are tilted with respect to the macrocycle and induce a deformation of the latter.¹¹ In addition, localized interactions between porphyrins' functional groups and the surface can influence the adsorption geometry. An example is the chemical bond between the central iminic nitrogen atoms (-N=) of a free-base porphyrin and copper surfaces that causes the imine groups to bend towards the surface while the molecule is strongly deformed.^{15,16,17} In conclusion, it can be stated that adsorbed porphyrin molecules adopt a conformation that is influenced by both the molecular structure and molecule-surface interactions. Furthermore, molecule-molecule interactions can play a role for determining the most stable conformation.¹¹

On weakly interacting surfaces like Au(111) and Ag(111), free-base porphyrins are usually mobile at room temperature. As a consequence, they form self-assembled structures consisting of well-ordered, square unit cells governed by molecule-molecule interactions.^{15,18} On Cu(111), a stronger interacting substrate, the iminic nitrogen-copper bond leads to strong, localized molecule-surface interactions and consequently immobilized molecules that do not form ordered islands at low to medium coverages.

Metalloporphyrins generally bind weaker to substrates than their free-base counterparts and therefore exhibit a higher mobility owing to a weaker nitrogen-substrate bond as the nitrogen atoms are coordinated to a metal center.^{11,19,20} For metalloporphyrins with a reactive metal ion center such as Co^{2+} or Fe^{2+} , charge donation from metal substrates to the central ions has been observed, resulting in a formal reduction of the metal center.^{21,22}

At the time when this thesis was started, only few studies had targeted porphyrin adsorption on oxide surfaces. In the meantime, on rutile $\text{TiO}_2(110)$, free-base tetraphenylporphyrin (2HTPP) as well as NiTPP were found to be immobile at room temperature, owing to a strong interaction with the oxygen rows of the substrate; 2HTPP was protonated to form 4HTPP^{2+} , either by surface hydroxyl groups or hydrogen diffusing out of the bulk.^{23,24} Copper(II)-phthalocyanines, which are structurally very similar to copper-porphyrins, showed on the other hand a weak interaction with Al_2O_3 thin films, resulting in a high lateral mobility and comparably low desorption temperatures.²⁵ For iron(II)-phthalocyanine on MoO_3 , XPS and NEXAFS measurements indicated a localized Fe-O bond and a charge transfer from the molecule to the surface.²⁶

The limited availability of data on oxide/porphyrin interfaces does not allow for the recognition of general patterns in the adsorption behavior yet. Therefore, more studies targeting this field are desired. One main goal of the work at hand was to fill the knowledge gap and provide more understanding of how porphyrins interact with oxide surfaces.

However, not only adsorption and surface interaction are interesting fields of research. Chemical reactivity, especially metal center insertion into the macrocycle and metal exchange can provide valuable opportunities to tune the molecule's functionality and should therefore be targeted as well.

1.2 Porphyrin metalation: homogeneous liquids vs metal surfaces

The metal center of the porphyrin is crucial for the functionality of the molecule since it can not only influence the electronic structure of the macrocycle, but also act as an active site for, for instance, the adsorption of small molecules²⁷ or catalytic reactions.¹⁰ Thus, controlling metalation, demetalation and metal center exchange are important steps for tailoring the functionality of porphyrins and have been studied extensively in liquid medium,^{28,29,30,31,32} but recently also on metal surfaces in ultrahigh vacuum.^{33,34} However, the reaction mechanisms in homogeneous solution and at the solid/vacuum interface are considerably different. In solution, ionic reactants, intermediates and products are favored due to solvent stabilization whereas in the absence of solvents, on metal surfaces in vacuum, reactions proceed preferably through neutral species. Figure 2 shows reaction schemes of the porphyrin metalation reaction in homogeneous solution (a), where the reaction proceeds as the replacement of two protons with a metal ion, and at the metal/vacuum interface (b) where the reaction follows a redox mechanism with the oxidation of a metal atom and the related reduction of two protons to form molecular hydrogen. The source of metal centers are dissolved metal ions in case a), and codeposited metal atoms such as iron¹⁸, nickel¹⁹ or zinc,³⁵ or substrate atoms from a reactive surface, e.g. Cu(111) in case b).³⁶

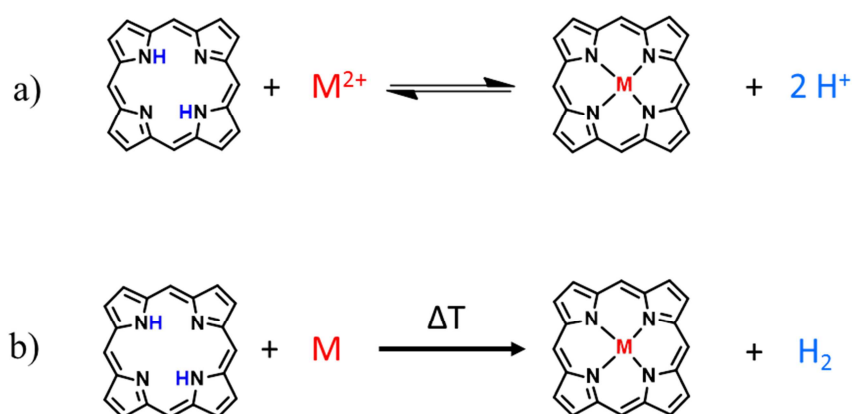


Figure 2. The mechanism of porphyrin metalation a) in homogeneous solution and b) at solid/vacuum interfaces

The second major goal of this thesis was to combine these two approaches and investigate whether the liquid phase approach can be also used to synthesize metalloporphyrins on surfaces.

2 Experimental methods

In the following chapter, the experimental methods which have been used to obtain the results within this thesis will be introduced briefly. The most important techniques were X-ray Photoelectron Spectroscopy (XPS) and Ultraviolet Photoelectron Spectroscopy (UPS), but also Temperature-Programmed Desorption (TPD) was applied.

2.1 X-Ray Photoelectron Spectroscopy (XPS)

The very first step towards paving the way for X-ray Photoelectron Spectroscopy (XPS) as a surface analysis method was taken by Albert Einstein when he discovered the photoelectric effect in the beginning of the 20th century.³⁷ About 60 years later, Kai Siegbahn developed the first photoelectron spectrometer based on Einstein's findings.³⁸

2.1.1 XPS basics

Figure 3 shows the basic principle of XPS: if a sample is irradiated with X-rays of sufficient energy, core electrons from the atoms of the specimen are excited and escape into the vacuum with a kinetic energy E_{kin} , which is measured by an analyzer.

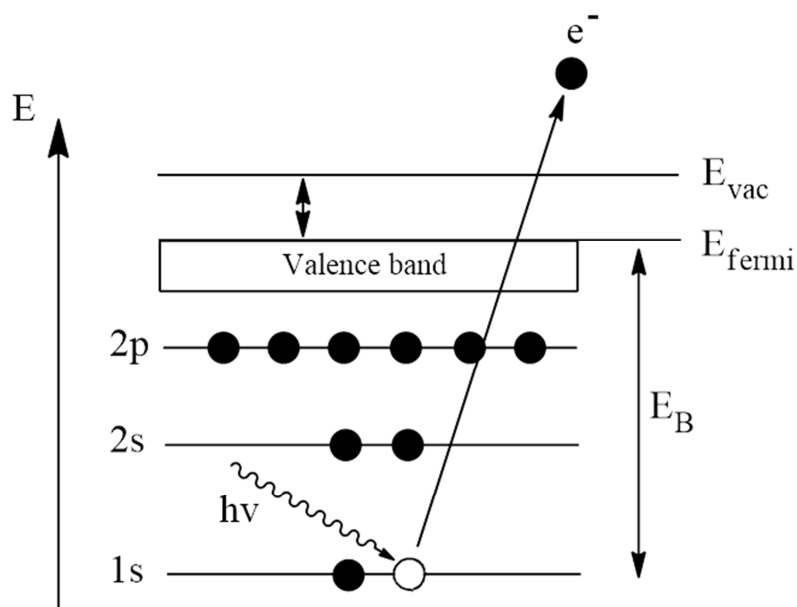


Figure 3. Schematic sketch, showing the energy levels of an atom and the principle of XPS

The relationship between E_{kin} of an electron and its original binding energy, E_B , is given as follows:

$$E_B = h\nu - E_{\text{kin}} - \Phi_{\text{Analyzer}},$$

$h\nu$ is the energy of the incident X-Rays, and Φ_{Analyzer} is the work function of the analyzer. The X-rays used as excitation source for the experiments in this thesis originated from a monochromatized aluminum X-ray source, utilizing the characteristic K_α radiation (1486.6 eV); or from a synchrotron light source. One of the advantages of XPS is that it is an element sensitive method; different elements can be distinguished by the binding energy of their core levels. X-rays penetrate several micrometers into the sample, but due to inelastic interactions of the released electrons with the atoms of the specimen, the inelastic mean free path λ of emitted photoelectrons amounts only a few nanometers. Therefore, XPS is a surface sensitive technique. However, if the excitation energy is fixed like in a conventional X-ray source, the information depth is not the same for all photoemission lines. The inelastic mean free path of the released electrons strongly depends on their kinetic energy and exhibits a minimum for electron energies between ~20-200 eV.³⁹ In synchrotron experiments, the excitation energy is usually adjusted for each XPS region separately so that all lines appear at the same kinetic energy of about ~100-150 eV. This leads to a high surface sensitivity and can facilitate data analysis. For example, if a photoemission line of an adsorbate cannot be clearly identified in a lab experiment because it is superimposed by signals from the substrate, synchrotron measurements enhance the adsorbate signal while depleting the background signal so that the adsorbate signal can be analyzed properly.

2.1.2 The XP spectrum

A photoelectron spectrum is usually obtained by plotting the number of detected electrons versus their binding energy. As an example, Figure 4 shows a spectrum of a clean Au(111) crystal, obtained with a monochromatic Al K_α X-Ray source.

Peaks from the 4p, 4d and 4f core levels are observed, in addition to the valence band structure, which will be explained in the chapter about Ultra Violet Photoelectron Spectroscopy (UPS). In addition, a background increase towards the higher binding energy side of the spectrum is observed. This is due to photoelectrons that are scattered inelastically within the specimen and therefore escape with a lower kinetic energy than electrons that cross the solid/vacuum interface without energy loss.

Each of the detected core level signals in Figure 4 appears not as one single line, but is split up in two instead. This phenomenon is observed for all orbitals other than s-orbitals, and the reason behind it is spin-orbit coupling: the electron spins can be either parallel or antiparallel, resulting in different values for the total angular momentum j (noted in the index of the orbital), and therefore different binding energies. The intensity of every component is determined by the number of possible combinations of spin- and angular momentum that yield the same j value.

The number of possible combinations n can be calculated by $n = 2j + 1$. For instance, this results in an intensity ratio of 4 : 2 for Au 4p_{3/2} : Au 4p_{1/2}. The energy splitting of the lines is proportional to $1/r^3$, while r is the mean radius of the orbital.

A different effect is observed if the initial state already contains unpaired electrons. XPS on paramagnetic compounds results in multiplett splitting and consequently complicated peak structures, originating from different possible interactions of the core hole with the unpaired electron. Thus, multiple final states with different energies are possible.^{22, 40,41,42} This will become apparent in Chapter 4.2, when the cobalt metal center of CoTPP molecules is analyzed.

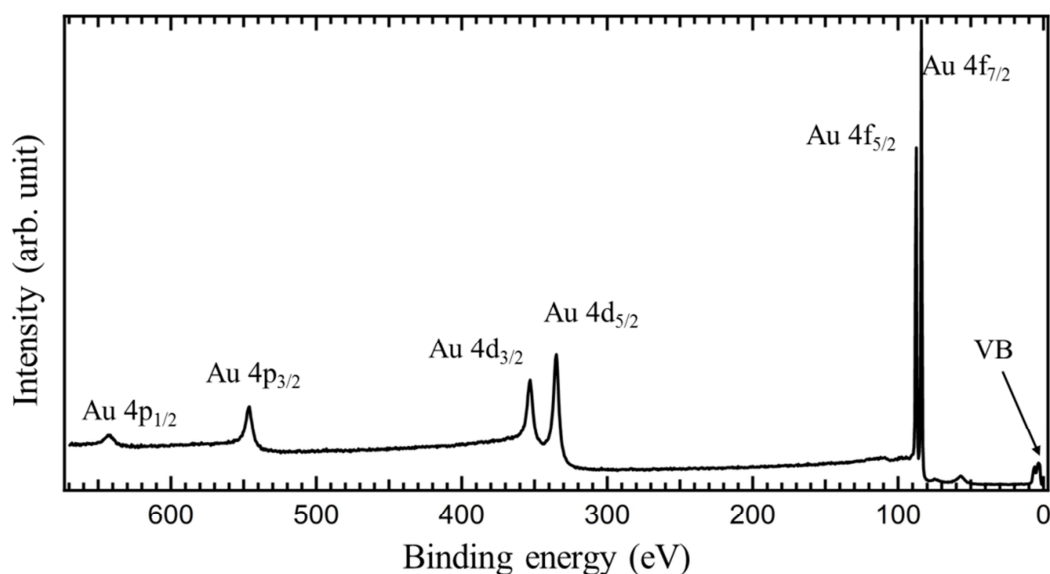


Figure 4. Overview XP spectrum, obtained from a clean Au(111) crystal

2.1.3 Core level shifts

XPS does not only allow for distinguishing between different elements, but is also sensitive to the chemical state of the element. Figure 5 shows the N 1s core level spectra of 2HTPP, ZnTPP and CuTPP, each 1 monolayer on Au(111), for comparison. In the 2HTPP spectrum, two different nitrogen species are present, namely aminic (-NH-) and iminic (=N-) nitrogens, splitted by 1.6 eV due to their different chemical environment. In ZnTPP, all four nitrogen atoms are equally coordinated to a Zn²⁺ metal center, therefore only a single peak appears, different in binding energy than the two species from the free-base molecule. The N 1s binding energy position of CuTPP is in turn by 0.3 eV different than that of ZnTPP, indicating the different metal center.

In this example, the binding energy shift is due to a change in valence electron density caused by the chemical environment of the atom, also denoted as chemical shift.

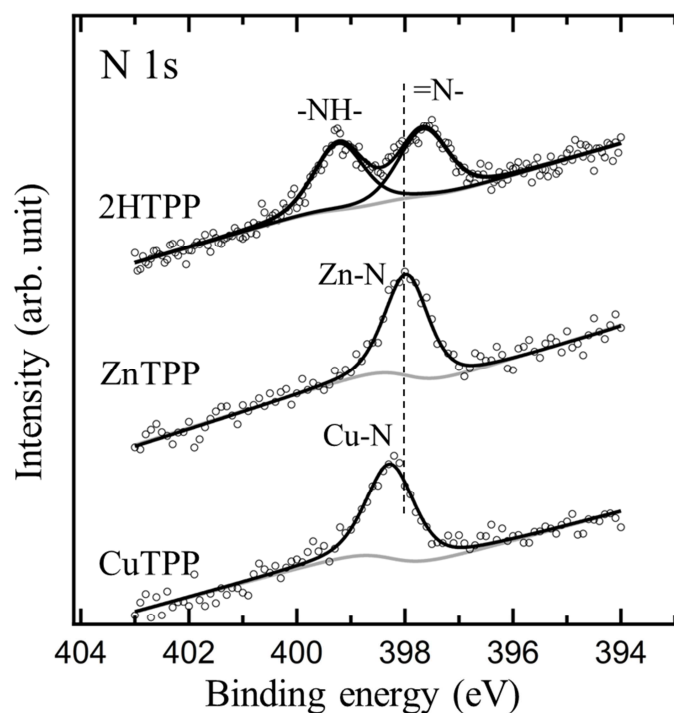


Figure 5. XP N 1s spectra of monolayers of 2HTPP, ZnTPP and CuTPP on Au(111)

Binding energy shifts can be also caused by so called final state effects, which are directly related to the process of photoemission. An example is final state screening on metal surfaces. If a core hole is created in close vicinity to a metal surface, the charge of the hole can be screened by free electrons in the metal and the final state is therefore stabilized, which leads to higher kinetic energies and, consequently, lower binding energies.

Herein, only a small selection of possible effects is described. For a more detailed examination, the reader is referred to the textbooks by Hüfner⁴³ and Briggs/ Seah.⁴⁴

2.1.4 Coverage determination with XPS

Not only qualitative information can be obtained by XPS, but also information about the quantity of elements present in the near-surface region is accessible. However, it has to be considered that the emitted electrons from deeper layers can interact inelastically with atoms from the bulk material and consequently lose energy. These electrons contribute to the background intensity but not to the main photoemission line, which leads to signal attenuation. According to Lambert Beers' law, the flux of unaltered photoelectrons travelling through solid decreases exponentially with travelled distance. Therefore, the total electron intensity escaping from a homogeneous solid can be calculated by summing up the emitted electrons from all layers n between $n=1$ and $n=\infty$ and multiplying it with a factor that declines exponentially with the layer depth:

$$I_{total} = \sum_{n=1}^{\infty} I_0 e^{-\frac{nd}{\lambda \cos \vartheta}}$$

I_0 is the intensity without attenuation, d the distance between two adjacent layers and λ the previously mentioned inelastic mean free path. It determines the distance that electrons can travel until their intensity is reduced by a factor of $1/e$. ϑ is the emission angle of the electron relative to the surface normal and the term $nd/\cos\vartheta$ consequently describes the distance that an electron from layer n has to travel to reach the surface.

A typical situation in an XPS experiment within this thesis is that the surface of a single crystal substrate is covered with an overlying metal oxide or an organic film (Figure 6).

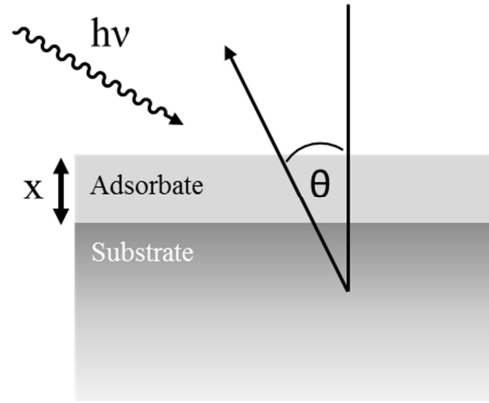


Figure 6. Substrate covered by an adlayer with thickness x .

In this case, the intensity originating from the overlayer, assuming layer-by-layer growth, is given by

$$I^{ad} = I_{\infty}^{ad} \left(1 - e^{-\frac{x}{\cos \vartheta \lambda_{ad}}}\right)$$

where x is the thickness of the overlayer film. I_{∞}^{ad} is the intensity that is obtained from an infinitely thick film of the adlayer. It can be approximated by an XPS experiment from a film that is so thick that the substrate signal is completely attenuated. In analogy, the substrate signal I^S is determined by

$$I^S = I_{\infty}^S e^{-\frac{x}{\cos \vartheta \lambda_{ad}}}$$

I_{∞}^S is the measured XPS intensity from the clean sample. Dividing the two equations by another, the ratio between I^{ad} and I^S can be calculated:

$$\frac{I^{ad}}{I^s} = \frac{I_{\infty}^{ad} (1 - e^{-\frac{x}{\cos \vartheta} \lambda_{ad}})}{I_{\infty}^s e^{-\frac{x}{\cos \vartheta} \lambda_{ad}}}$$

To determine λ_{ad} , I^{ad}/I^s has to be measured for a known coverage. One way to create a known coverage of an adlayer on a substrate is by measuring the growth rate with a quartz microbalance. This procedure was applied for the metal oxide thin films in this thesis. For porphyrin adlayers, a different method has been proven to be more accurate: one closed layer of porphyrins can be produced by covering the sample with multilayers of porphyrins and subsequently annealing it to 550 K for 5 minutes. During annealing, the multilayers desorb and the remaining carbon coverage is defined as 1 monolayer.

If λ_{ad} , I_{∞}^{ad} and I_{∞}^s are known, the thickness x of the adlayer can be calculated for every experiment from the experimentally determined I^{ad}/I^s .

2.2 Ultra-Violet Photoelectron Spectroscopy (UPS)

UV-Photoelectron Spectroscopy (UPS) is based on the principle of photoemission as is XPS. The difference is that UPS utilizes UV-light as excitation source, usually generated from Helium-discharge lamps, with an energy of either 21.2 eV (He-I line) or 40.8 eV (He-II line). It can also be conducted by using synchrotron radiation with adjustable energy. Due to the low excitation energy,

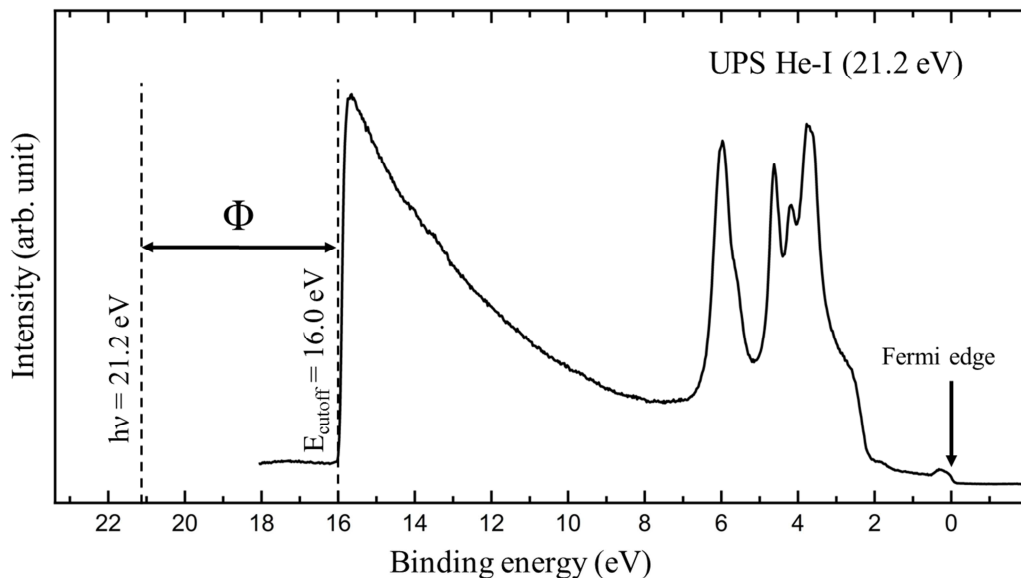


Figure 7. UP spectrum of a clean Au(111) single crystal

the electrons which are excited from the specimen are not core electrons, but originate from the valence band region. Since the valence orbitals are responsible for forming chemical bonds, UPS is a suitable tool for studying the electronic structure of molecules adsorbed on surfaces. In contrast to

XPS, UPS is not a quantitative method. The reasons for that are: a) the photoionization cross sections vary strongly between different energy levels for low excitation energies, and b) photoelectron diffraction effects start to play a role at low kinetic electron energies. Figure 7 shows a UP spectrum obtained from a clean Au(111) single crystal by using He-I light.

The difference between the excitation energy (21.2 eV) and the secondary electron cutoff (here at 16.0 eV) represents the work function of the sample (5.2 eV). In this thesis, UPS was used to obtain work functions and to gain information about molecule-substrate interactions by observing molecular states close to the Fermi edge.

2.3 Temperature-Programmed Desorption (TPD)

When it comes to the investigation of on-surface chemical reactions, Temperature-Programmed Desorption (TPD) has shown to be a valuable tool in combination with XPS measurements. In principle, the method works as follows: the sample is heated with a linear heating ramp while a mass spectrometer detects desorbing species. If the sample temperature is high enough to overcome a reaction barrier, any volatile products of the reaction desorb and are detected. Figure 8 shows an example of a desorption spectrum where mass 18 (water) was detected as a function of the temperature for a Ag(100) sample covered with 18 layers of an organic acid. The molecular structure of the organic acid, namely phthalic acid, is depicted in Figure 8. Four desorption peaks are detected, labelled from **a-d** in Figure 8. The most prominent feature, peak **b** at 180 K, was identified in combination with XPS measurements to be due to a chemical reaction of phthalic acid, producing phthalic anhydride and water (Figure 9). Phthalic anhydride remains at the surface at these low temperatures, but water immediately desorbs and can be detected by the mass spectrometer.

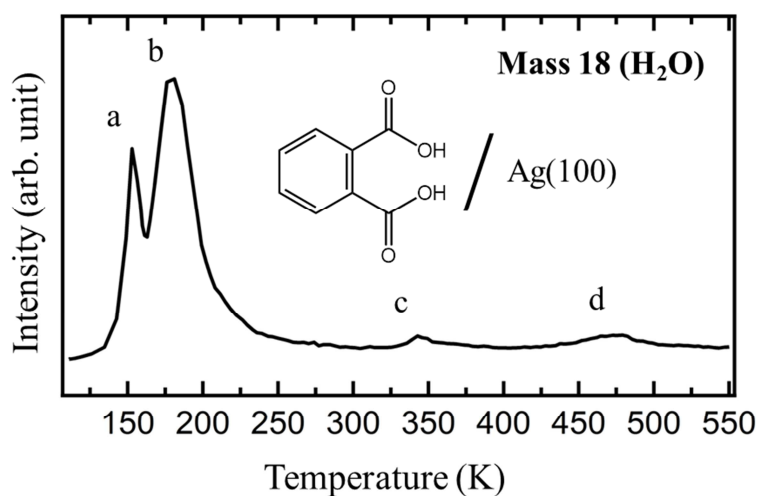


Figure 8. Desorption spectrum of mass 18 (water) from a Ag(100) sample covered by multilayers of phthalic acid.

However, not all desorption peaks are due to chemical reactions producing water. Peak **a** is attributed to adsorption of residual water on the low-temperature sample and peak **c** originates as part of the cracking pattern of desorbing phthalic acid multilayer molecules. Peak **d** indicates another chemical reaction: the decomposition of polymeric anhydride species which are formed as a side product of phthalic anhydride at 180 K.

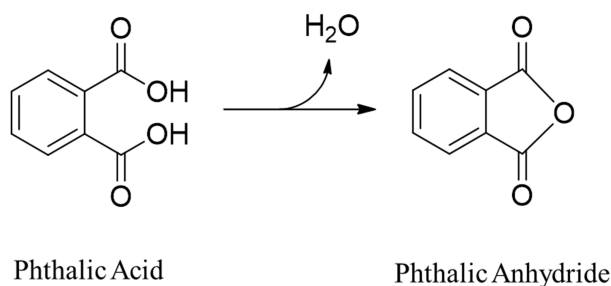


Figure 9. Conversion of phthalic acid into phthalic anhydride and water.

To minimize the detection of species desorbing from the backside of the sample, the heating wires and the sample holder, a setup with a Feulner Cup mounted around the ionization source of the mass spectrometer was used. The Feulner Cup is a copper cone with a 5 mm wide opening (sample diameter: 10 mm) which is approached approx. 1mm to the front of the sample during a TPD experiment. A detailed drawing of the experimental setup can be found in the PhD thesis of Michael Röckert.⁴⁵

TPD spectra can be used to obtain information about reaction kinetics. Different analysis methods have been developed to determine preexponential factors and activation energies from desorption spectra, all based on the Polanyi-Wigner equation.⁴⁶ These methods were not applied in this thesis and will therefore not be discussed here. The interested reader will find an a detailed examination within the articles of de Jong et al⁴⁷ and Falconer et al.⁴⁸

3 Experimental details

3.1 Setup

Most of the work in this thesis was conducted inside stainless steel ultrahigh vacuum (UHV) chambers with background pressures of below $4 \cdot 10^{-10}$ mbars. The vacuum is needed to keep the level of surface contamination low, especially when doing long-time measurements like XPS in the N 1s regions of low-coverage porphyrin layers as it was done for the experiments in [P3]. The main components of the residual gas in the chambers are H₂, H₂O, CO₂ and CO. While H₂ and CO₂ do not adsorb on the substrates used in this thesis (Ag(100), MgO(100) and Au(111)), H₂O can dissociatively adsorb on MgO(100), forming hydroxyl groups at room temperature.⁴⁹ CO adsorbs reversibly below 180 K⁵⁰ and CO₂ below 260 K upon formation of carbonate.⁵¹

When measuring at temperatures below 150 K, water adsorption from background gas occurs on any substrate. This has to be considered when doing measurements at low temperature, as it was done for phthalic acid on Ag(100) [P5]. If it is assumed that water contributes by ¼ to the background pressure, the water pressure in the chamber is around 10^{-10} mbar. To estimate the amount of water contamination on the sample, we can calculate the incoming flux of molecules I using the kinetic gas theory:

$$I [s^{-1}m^{-2}] = \frac{p}{\sqrt{2\pi \cdot T \cdot m_{mol} \cdot k_B}}$$

p is the partial pressure, T the temperature in K, m_{mol} the mass of the molecule and k_B the Boltzman constant. The numbers in our example give rise to a flux of $3.6 \cdot 10^{14} s^{-1}m^{-2}$, which means that $\sim 10^{11}$ water molecules impinge per second on a sample with 10 mm diameter. Within the time span of a few hours, a whole monolayer of water will be formed (assuming a sticking coefficient of 1), which means that even after 20-30 minutes at low temperature, water will be detected by sensitive methods like synchrotron radiation XPS.

In addition, experimental techniques relying on electron- and ion detection require pressures in the 10^{-6} mbar range or below to avoid collisions between electrons/ ions and residual gas molecules.

The experiments in this thesis were carried out in four different vacuum chambers: the home lab in Erlangen; Federico Williams's lab at the university of Buenos Aires, Argentina; the endstation of the Material Science Beamline at Elettra Synchrotron Trieste, Italy and the endstation of I09 beamline at the Diamond Light Source in the United Kingdom. All of these chambers are equipped with standard features for surface preparation and analysis: a moveable sample holder, radiatively heated evaporators, LEED optics and an ion gun for Ar⁺-sputtering. In addition, all of them have a hemispherical analyzer for photoelectron detection. The chambers in Buenos Aires and Erlangen work with monochromatized Al K_α X-rays and the beamline endstations with synchrotron light as excitation

sources. The home lab in Erlangen has an additional setup for TPD measurements (see Chapter 2.3), employing a Pfeiffer QMG 700/ QMA 400 quadrupol mass spectrometer which allows for detection of masses up to 2048 amu. The special feature of the chamber in Buenos Aires is a teflon cell (detailed description in Chapter 3.2.2) in which UHV-prepared samples can be exposed to liquids in an argon atmosphere.

3.2 Sample preparation

The sample was cleaned with consecutive cycles of Ar⁺-sputtering and annealing. The term sputtering denotes that gas atoms (usually noble gases) are ionized and accelerated towards the sample. Upon impinging on the sample, ions remove the topmost layers of the surface. This reduces the amount of impurities on the surface, but also creates a rough surface morphology. The argon pressure in the chamber was kept at around $5 \cdot 10^{-6}$ mbar; ion energies of 1 and 0.7 keV were used for the Au(111) and Ag(100) single crystal surfaces, respectively. The reason why 0.7 keV ion energy was not exceeded for Ag(100) is that the (100) surface of silver is not thermodynamically stable and will form (111) facets if sufficient activation energy is provided. After ion bombardment, the single crystals were annealed for 15 minutes to 700 K (silver) and for 5 minutes to 1000 K (gold). Annealing provides thermal energy for the atoms of the specimen whose mobility increases and a flat surface is formed to minimize surface energy. The preparation of well-defined MgO(100) surfaces is covered in a separate chapter (3.2.1).

Organic molecules were deposited by thermal evaporation from quartz- or graphite crucibles of radiatively heated evaporators. This requires thermal stability of the molecules up to temperatures above the evaporation temperature, which was the case for all molecules used in this thesis. 2HTPP free-base porphyrins were evaporated at temperatures around 600 K with a deposition rate of ~0.2 monolayer/min and metalated porphyrins (ZnTPP, CuTPP and CoTPP) at 620-630 K and similar deposition rates. Phthalic acid was evaporated at 400 K (0.5 monolayer/min) and phthalic anhydride at room temperature.

3.2.1 MgO thin film growth

The aim of the experiments within [P3] and [P4] was to investigate the adsorption and reaction of molecules on MgO surfaces. Since photoelectron spectroscopy requires conductive samples and MgO is an insulator, MgO single crystal cannot be used for XPS and UPS. Instead, thin films of MgO were grown on a metallic substrate, namely Ag(100), to ensure sufficient conductivity.

Ag(100) is a convenient substrate to grow MgO, since the lattice mismatch between MgO and silver is small (2.9%). In addition, the combination of the hard oxide and the soft metal enables the

shift of misfit dislocations into the metal which leads to well-ordered oxide films at low coverages.^{52,53} There are different ways to grow MgO on Ag(100). Either, metallic magnesium is deposited first on the substrate and then post-oxidized by O₂ exposure, or O₂ is dosed simultaneously while magnesium is evaporated onto the sample. Among these two methods, the post-oxidation method was shown to result in films of worse quality due to a significant amount of unoxidized metallic magnesium as well as non-stoichiometric oxide species.⁵² For this reason, the simultaneous oxidation method was chosen for this thesis. Within our research unit (functional organic molecules on complex oxide surfaces - funCOS), different research groups experimented with the growth parameters and the following recipe was found to produce good quality films.

Magnesium was evaporated at a rate of ~1 monolayer/min in an atmosphere of 10⁻⁶ mbar O₂ at 630 K from a stainless steel crucible while the sample was kept at 450 K. The evaporation rate was measured with a quartz microbalance. After growth, the films were annealed to 650 K in 10⁻⁶ mbar O₂ for 5 minutes to improve their order. The quality of the films was judged with LEED and XPS after preparation. XPS confirmed the absence of impurities (apart from a small carbon impurity at 283.0 eV binding energy, presumably magnesium carbide), while LEED gave an impression on the overall ordering of the film. A typical LEED pattern of a 10 monolayer MgO(100) film, obtained at 96.5 eV, is shown in Figure 10. It shows the typical 1x1 pattern with four-fold symmetry.

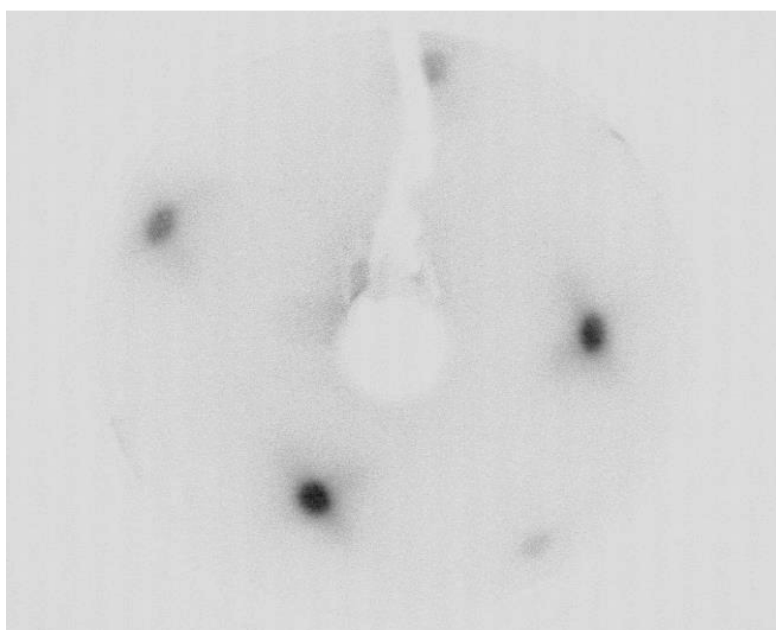


Figure 10. LEED pattern of ~10 monolayer MgO, grown on Ag(100), obtained at 96.5 eV.

An important question when doing experiments on MgO is the right thickness of the films to aim for. Very thin MgO films (~1-2 monolayers) show the best ordering, but are different to bulk MgO concerning their electronic properties. Layer-resolved conductance measurements showed that at least 3 layers of MgO are needed to obtain an electronic structure similar to that of bulk MgO (band gap of

~ 6 eV).⁵⁴ Since in this work, thin film MgO was used as a model system for bulk MgO, the properties of the grown thin films should be ideally the same as for bulk MgO. Another challenge is posed by the similar surface energies of silver (1.30 J/m^2) and MgO (1.16 J/m^2).⁵³ At lower oxide coverage, the probability of silver atoms diffusing through the MgO film and reacting with deposited molecules is higher than at high coverage. Too thick films on the other hand show worse ordering and poor conductivity, the latter being crucial for photoelectron spectroscopy. Taking all advantages and drawbacks of thin and thick films into account, the thickness of the MgO films was kept between 5 and 10 monolayers in this thesis.

3.2.2 Liquid phase experiments

One part of the experiments in this thesis ([P1] and [P2]) included exposing porphyrins adsorbed on Au(111) single crystals to aqueous solution. To do so, the vacuum chamber in Prof. Federico Williams' group at the University of Buenos Aires has a special experimental setup. First, the sample was transferred to a load lock chamber that can be separated from the main chamber. Subsequently, the load lock was vented with argon and a valve at the bottom of the load lock was opened to move the sample downwards into an argon-purged Teflon cell. The aqueous solution was injected with a syringe from the bottom of the cell. Figure 11 shows a schematic drawing of the procedure how the samples were exposed, exemplified with a metalation reaction of free-base porphyrins. The crystal (1) was dipped head first into the metal ion-containing solution and slightly pulled back so that a meniscus was formed (2). After a certain exposure time, the crystal was removed from solution, leaving a drop of solution still adhering to the surface (3). The drop was rinsed with 50 ml of neutral, distilled water. The remaining drop of neutral water was then blown away by an argon stream, leaving only a thin liquid film on the sample behind (4) which was dried before the sample was transferred back into the load lock chamber. After that, XPS and UPS measurement were conducted on the specimen. A major challenge during these experiments was to avoid contamination of the surface by undesired, dissolved organic species, as all non-volatile contaminants present in the liquid film at step (4) are deposited on the surface as the liquid dries. Therefore, even low contaminant concentrations in solution can cause considerable contamination on the surface. For example, if a water film thickness of 1 mm is assumed, the contaminant concentration in solution which is needed to cover 2-3% of the surface is in the low 10^{-5} M range. Therefore, a lot of attention has to be paid to the method of water purification (Chapter 3.3).

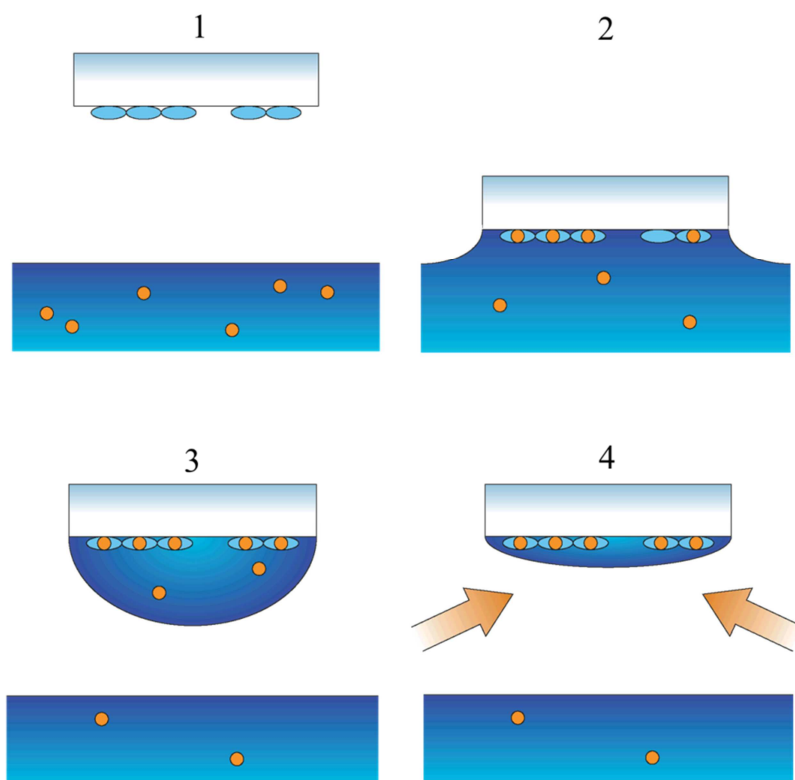


Figure 11. Schematic drawing how porphyrins on a single crystal are exposed to aqueous solution.

3.3 Water purification

It is crucial to minimize nitrogen-containing contaminations if a detailed measurement on the XPS N 1s region is desired, for instance when investigating the metalation of porphyrins. As XPS is a very sensitive method, even small contaminations of about 2-3 % surface coverage are easily visible. Different methods of water purification for the liquid phase exposure experiments were applied, and the results can be seen in Figure 12. In the first experiments, twice-distilled and subsequently deionized water was used, which led to a significant amount of nitrogen and carbon contamination (Figure 12a), presumably due to dissolved organic species. Inorganic contaminations can be excluded since the water was previously deionized. The binding energy position of the additional nitrogen species is consistent with organic amines. The second approach was to distill the treated water from a KMnO_4 solution. Upon heating, the organic species should be oxidized by MnO_4^- to form volatile oxides. As evident from Figure 12b), this approach led to much less contamination in the nitrogen region, but even higher carbon contamination. A possible explanation is that even though most of the nitrogen-containing organic species have been oxidized, new impurities have been picked up from the distillation column or from air.

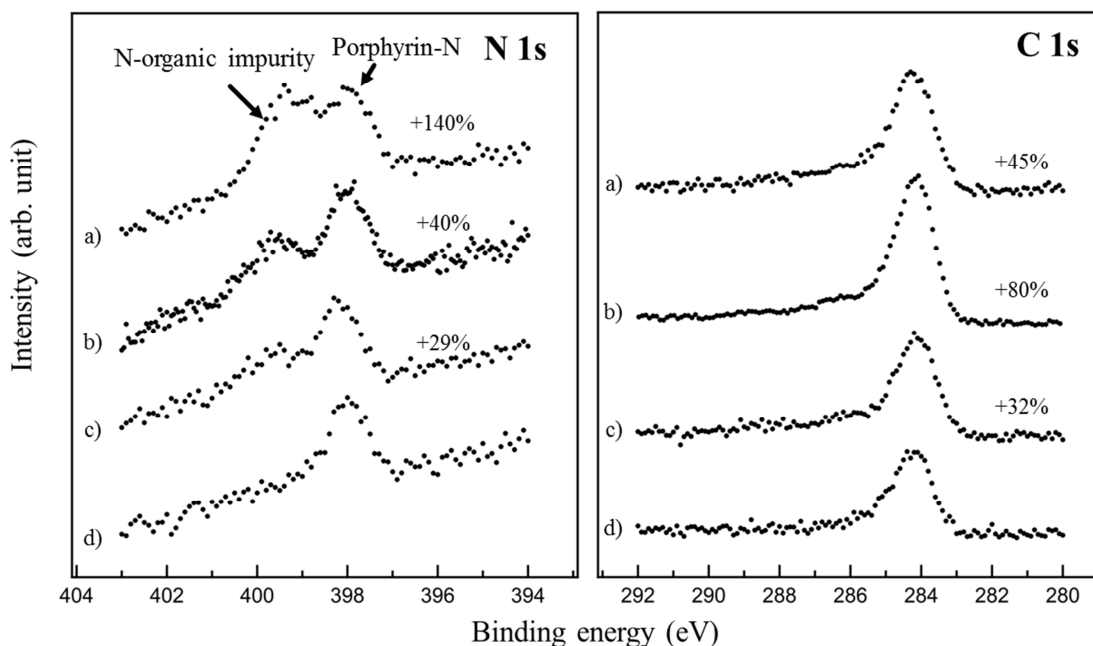


Figure 12. N 1s and C 1s regions of 1 monolayer ZnTPP a) exposed to twice-distilled and deionized water, b) after the water has been distilled from a KMnO_4 solution and c) treated with UV light under argon atmosphere. d) shows the unaltered spectrum as a reference.

The third approach was to irradiate the treated water for 1 hour with UV-light in Argon atmosphere. Figure 12c) shows the result: among the three methods, the UV irradiation has resulted in the least contamination in the carbon as well as in the nitrogen region. Upon irradiation, OH radicals are formed which oxidize dissolved molecules and therefore result in a higher water purity. The total organic content of the water was determined by measuring the chemical oxygen demand to be lower than 60 ppb after UV treatment. Figure 12d) shows a spectrum of ZnTPP as deposited as a reference. No buffered solutions were used in these experiments to avoid potential contaminants.

4 Results

The experiments in this thesis can be divided into two major topics: porphyrins at solid/liquid interfaces and porphyrin adsorption on thin MgO films. In addition, anhydride formation of phthalic acid on a silver surface was investigated.

4.1 Porphyrins at solid/liquid interfaces

The articles [P1] and [P2] were published based on results obtained in the surface chemistry group of Federico Williams in Buenos Aires, Argentina.

The main purpose of the experimental work was to find out whether porphyrins adsorbed on a solid surface exhibit the same reactivity as porphyrins in homogeneous solution. To address this question, three test reactions which were studied extensively in liquid medium^{28,29,30,31,32} were conducted with porphyrins adsorbed on a Au(111) surface. The three test reactions are displayed in Figure 13: a) metalation of 2HTPP free-base porphyrin with dissolved Zn^{2+} ions, b) metal center exchange of Zn(II) metal centers with Cu(II) ions and c) demetalation of ZnTPP in acidic solutions. All of the above-mentioned reactions proceed through ion exchange mechanisms.

a) Metalation:



b) Metal center exchange:



c) Demetalation:

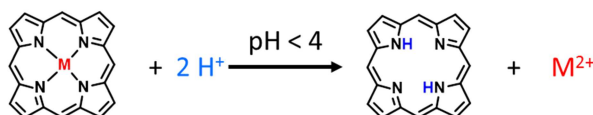


Figure 13. The 3 test reactions which were attempted with surface porphyrins in the framework of this thesis.

Noteworthy, metalation of surface porphyrins in vacuum has already been conducted and is – opposed to the ion exchange mechanism in liquid phase - known to proceed through a redox reaction in which a metal atom is oxidized and incorporated into the macrocycle, while the central protons are reduced to form molecular H_2 .^{34,35} To our knowledge, there is only a single surface science study published on

porphyrin metal center exchange,³³ which also proceeds in a redox reaction, and no study on demetalation yet. To induce the reactions, porphyrin layers deposited on Au(111) were exposed to aqueous solutions according to the procedure described in Chapter 3.2.2.

Metalation [P1] was attempted by exposure of one monolayer of 2HTPP to 0.7 M zinc acetate solution at room temperature for 2 h. The XPS results are displayed in Figure 14. Before exposure (b), the N 1s region of 2HTPP is characterized by two equal-area peaks, representing the central aminic (-

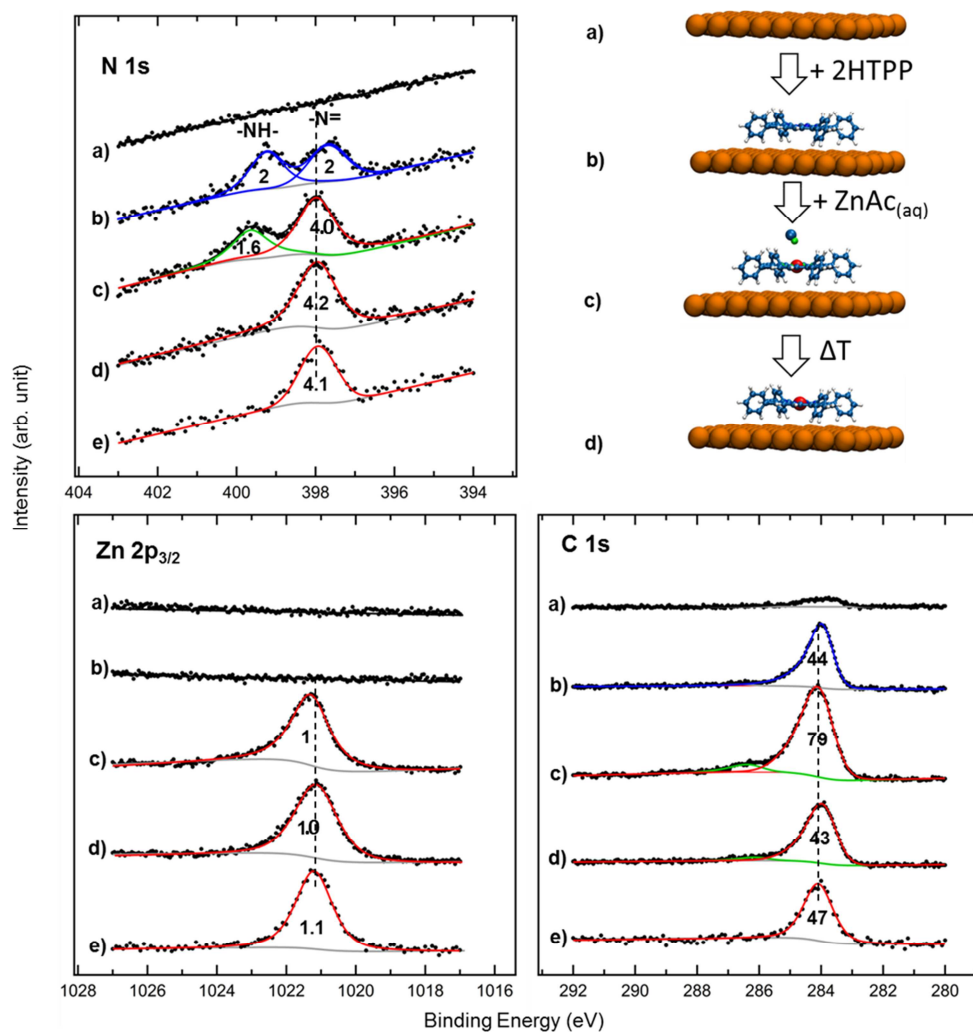


Figure 14. XP spectra of the N 1s, Zn 2p, and C 1s regions of (a) the clean Au(111) surface, (b) after 1 monolayer preparation of 2HTPP, (c) after exposing the 2HTPP monolayer with 0.7 M ZnAc₂ solution for 2 h, (d) after subsequent -annealing to 523 K for 5 min, and (e) 1 monolayer ZnTPP on Au(111) reference spectrum.

NH-) and iminic (-N=) nitrogen atoms, which is characteristic for free-base porphyrins. After exposure (c), a new feature (red) appears, located between the two free-base signals in binding energy and with the combined area of the two, strongly indicating that metalation took place. This significant change is accompanied by the depositon of zinc on the surface, as evident from the Zn 2p_{3/2} signal. However, another feature in the N 1s region (green) is detected at lower binding energy, which has no

counterpart in the spectrum obtained before exposure. In addition, the C 1s intensity increases by ~80%. These two observations are due to coadsorption of nitrogen-containing organics during exposure to the liquid, as described in Chapter 3.3. Upon annealing the sample in vacuum to 523 K for 5 min, the contamination desorbs (d) and spectra are observed which agree very well with deposited ZnTPP (e). Thus, it can be stated that the liquid phase synthesis approach has been successful on the surface. UPS measurements (not shown here, see [P1]) resulted in very similar spectra for 2HTPP before and after metalation. A minor difference is the presence of a low-intensity feature at ~0.9 eV below the Fermi edge before metalation which disappears upon Zn²⁺ coordination. It is speculated that this is due to localized iminic nitrogen – surface interaction that is weakened upon N-Zn bond formation.

A similar exposure experiment was also conducted with multilayers (~ 3 monolayers) of 2HTPP, resulting in a complete metalation, presumably because zinc ions are able to diffuse into the multilayers.

After it has been shown that metalation from solution is possible, the next step was to conduct a metal center exchange. Exchanging Zn(II) with Cu(II) metal centers in TPP's has been shown to be achieved easily in aqueous solution due to the high stability of CuTPP,²⁸ therefore the same exchange was attempted in this thesis [P2]. ZnTPP monolayers deposited on Au(111) were exposed for 1 h at room temperature to aqueous CuSO₄-solutions of different concentrations. The starting point, the ZnTPP monolayer, is displayed in the center of Figure 15 (a). After it has been exposed to 6 μM CuSO₄ solution, the peak area in the Zn 2p_{3/2} region has decreased by ~90% , consistent with a loss of the metal center (b). The N 1s region still consists of a single peak, apart from a small impurity peak that has been observed previously (Figure 14), which indicates a metalated and not a free-base species. Simultaneously, a new signal in the Cu 2p_{3/2} region appears. Comparing the spectra with reference spectra of a deposited CuTPP monolayer on Au(111) (e) shows that indeed CuTPP has been produced. The N 1s signal is shifted by +0.3 eV to the binding energy position consistent with the CuTPP reference spectrum.

We furthermore exposed the ZnTPP monolayer with a higher CuSO₄-concentration, namely 1 mM (Figure 15c). The spectra show that the Zn 2p_{3/2} signal now disappears completely, whereas a higher degree of nitrogen impurities are detected. Furthermore, another peak in the Cu 2p_{3/2} region is visible at 932.0 eV binding energy, consistent with Cu(0), probably due to underpotential deposition of Cu,⁵⁵ and the Cu²⁺ peak is larger than expected. The latter could be due to additional CuSO₄ that has not been rinsed away completely. Upon vacuum annealing to 523 K for 5 min, all impurities are removed and a clean layer of CuTPP is yielded (d).

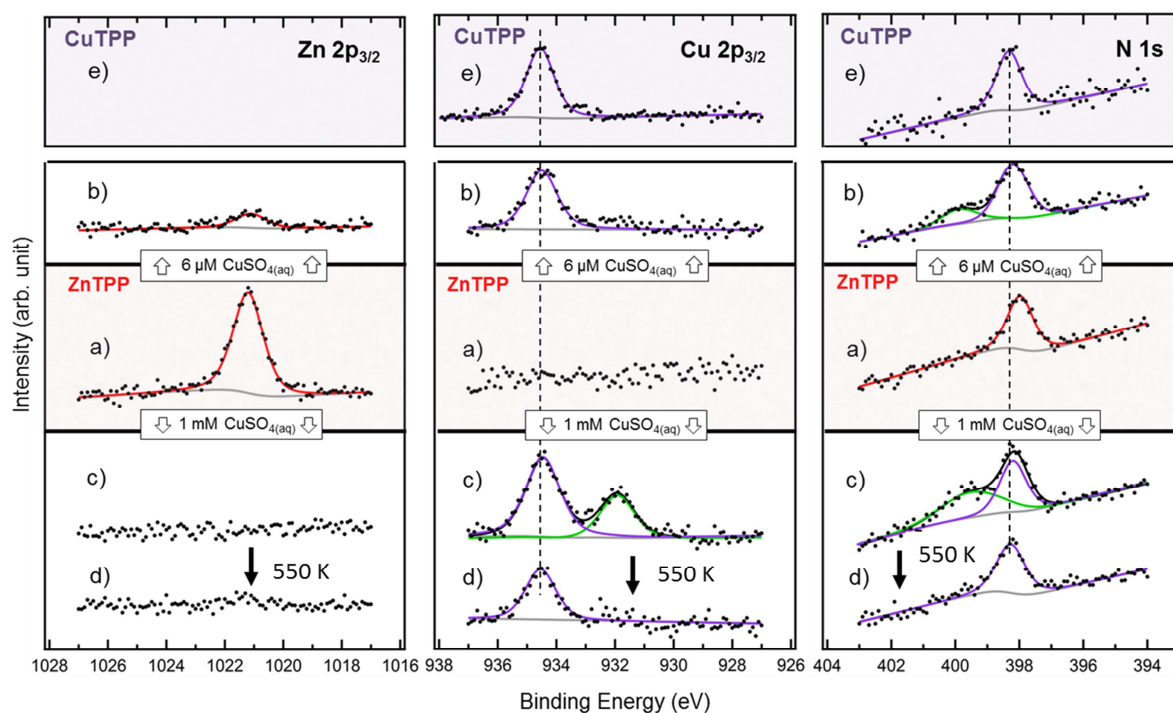


Figure 15. XPS spectra of the Zn $2p_{3/2}$, Cu $2p_{3/2}$, and N $1s$ regions of 1 monolayer ZnTPP after deposition on Au(111) (a) and after exposure to an aqueous solution of either b) $6 \mu\text{M}$ or c) 1 mM CuSO_4 at room temperature for 1 h. Included is also the spectrum after annealing the sample exposed to the 1 mM solution to 523 K for 5 min (d), and, as a reference, the spectra of one monolayer of CuTPP as deposited on Au(111) (e).

As a mechanism for the ion exchange, we propose a similar pathway to that in solution (Figure 16).²⁸ Throughout the exchange, an intermediate is formed that coordinates both the incoming and outgoing ion out of the macrocyclic plane (b). The surface could act as a ligand for the outgoing ion, as displayed in Figure 16.

To test if the ion exchange is reversible we exposed one monolayer of CuTPP adsorbed on Au(111) to a 10 mM aqueous solution of zinc acetate, but no exchange was visible in XPS (data not shown).

Since we have confirmed that metalation as well as ion exchange at the solid/liquid interface is possible as it is in homogeneous solution, the next step was to attempt demetalation. At pH values below 4 in solution, the Zn(II) metal center can be removed from ZnTPP, yielding metal-free porphyrins.²⁸

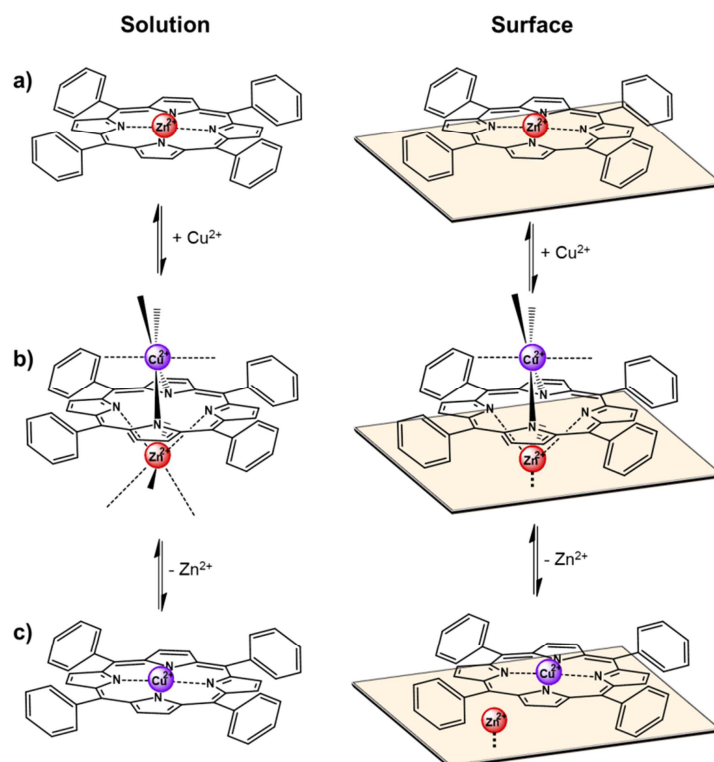


Figure 16. A suggestion for an ion exchange mechanism on the surface, where the surface acts as ligand for the outgoing ion.

This led us to perform an experiment where we exposed 1 monolayer of ZnTPP to an acidic solution of trifluoro-acetic acid (CF_3COOH) of $\text{pH}=1$ for 1h at room temperature. The XPS results are shown in Figure 17. The top chart (a) shows the initial spectrum of ZnTPP and (b) the spectrum obtained after exposure. For comparison, a reference spectrum of free-base 2HTPP is displayed in the bottom chart (c). Obviously, demetalation did not occur as evident from the Zn $2p_{3/2}$ signal which is still present. Also the N 1s signal still consists of a single peak after exposure (plus the expected impurity peak at lower binding energy), and not of two peaks as for a free-base molecule. Even though the reaction product expected in solution would be a porphyrin diacid (4HTPP^{2+}), we expect to see 2HTPP in XPS because we rinsed the crystal after exposure with neutral water. Even at $\text{pH}=0$ (results not shown), no indication of demetalation was present, instead the amount of impurity deposited on the sample increased.

As metalation and metal center exchange occurred at the solid/liquid interface just as expected from previous studies in homogeneous solution but demetalation did not, the need for a mechanistic explanation arises.

Most but not all literature on the demetalation mechanism agrees that it proceeds through a specific intermediate, the sitting-atop complex (Figure 18b) left).^{56,57,58} In the sitting-atop complex, the metal atom is located out of the porphyrin plane, while being coordinated to two of the central nitrogen atoms and four water molecules. The other two nitrogen atoms are protonated with the

protons in *trans*-position with respect to the metal center. For ZnTPP adsorbed on Au(111), a zinc-surface bond could be formed. It is possible that the sitting-atop complex on the surface is therefore stabilized significantly relative to the free-base reaction product.

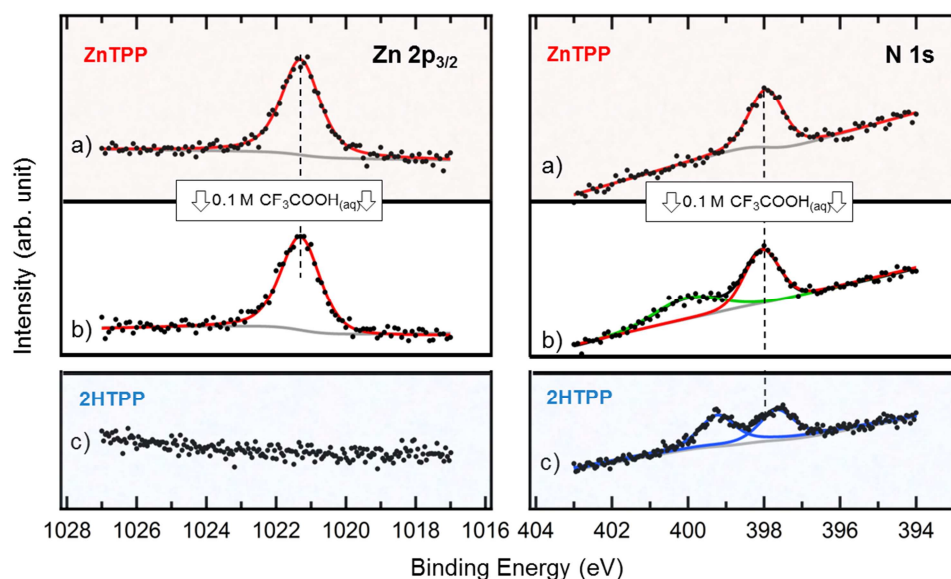


Figure 17. XPS spectra of an attempt to demetallate one ZnTPP monolayer on Au(111) (a) by exposure to acidic solution (pH=1) (b).

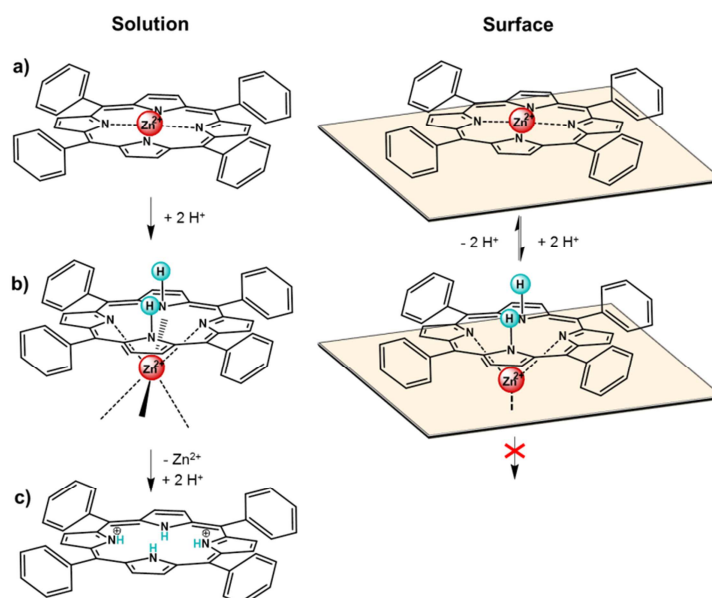


Figure 18. The demetalation mechanism of porphyrins in solution (left), forming a protonated porphyrin diacid, and our suggested model for the surface reaction (right), stopping at the SAT complex.

If this is the case, the sitting-atop complex could be the stable form in acidic solution. As the crystal is rinsed with neutral water after exposure, the sitting atop complex would be deprotonated and the initial molecule, ZnTPP, yielded and detected in XPS.

4.2 Porphyrin adsorption and reactions on MgO thin films

To address the second goal of the thesis, the adsorption and reactions of porphyrins on oxide surfaces, 2HTPP [P3] as a prototype free-base porphyrin and CoTPP [P4] as an example of a metalated porphyrin were deposited on thin MgO films which were grown according to the procedure described in Chapter 3.2.1. The article [P3], investigating the adsorption and reactions of 2HTPP on MgO thin films was part of a funCOS-cooperation with Prof. Oliver Diwald's group from the Department of Material Science and Physics at the University of Salzburg, who did similar measurements on MgO nanocubes.

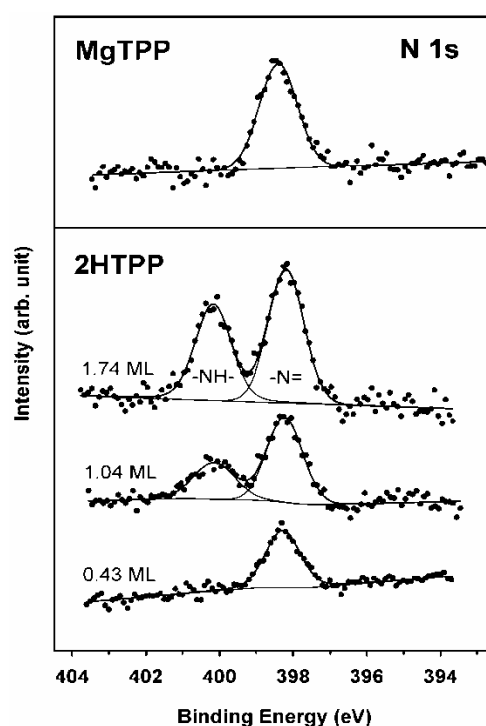


Figure 19. XPS measurements of different 2HTPP deposited on MgO thin films at room temperature and, as a reference, MgTPP on MgO.

The measurements were also complemented with calculations from the group of Prof. Bernd Meyer from the Computer Chemistry Center in Erlangen. Figure 19 shows room-temperature XPS N 1s measurements of different 2HTPP coverages on a 10 monolayer MgO film conducted with a monochromatized Al K_{α} X-ray source in our home lab in Erlangen.

Surprisingly, the low-coverage spectrum shows a single peak in the N 1s region and not the two well-separated, equal area peaks that would be expected for a free-base molecule. As discussed previously, four equivalent nitrogen atoms in a porphyrin molecule indicate a metalated species. It is known from several studies that tetrapyrrole molecules can metalate with surface atoms on certain metal substrates,^{36,59} but self-metalation has never been observed on oxide surfaces yet. Since MgTPP is

known to be a stable molecule which can be also found in nature,⁵ the possibility that 2HTPP could react with substrate-Mg²⁺ ions to form MgTPP has to be considered. Indeed, if MgTPP is deposited on MgO (top spectrum of Figure 19), the binding energy position of the N1s signal matches with that obtained after depositing low coverages of 2HTPP. As more molecules are deposited, a second peak appears at the binding energy of an aminic nitrogen (-NH-) of a free-base porphyrin and both peaks increase simultaneously with coverage. Therefore, we conclude that only molecules up a coverage of ~0.5 monolayer are metalated and further deposited porphyrins remain in their free-base form.

As described in Chapter 1.2, the self-metalation on metal surfaces proceeds through the oxidation of a metal atom from the surface and the reduction of the central protons inside the porphyrin's central cavity. On MgO, no metallic species are present. Therefore, we suggest that the reaction proceeds through an ion exchange, similar as it is known to be the case in liquid phase reactions. Table 1 shows calculated energy changes for reactions between 2HTPP and Mg²⁺ ions forming MgTPP and two OH groups at different surface sites. The calculations stem from Martin Gurrath and Bernd Meyer from the Computer Chemistry Center in Erlangen.

	Corner	Edge	Step	Terrace
$\Delta E_{met}^{hyd} [eV]$	-1.65	-1.13	-1.52	+0.51

Table 1. Calculated energy changes for the MgTPP- and hydroxyl group formation at different surface sites.

At terrace sites, the reaction is slightly endothermic, whereas it spontaneously happens at corner, edge and step sites. We therefore conclude that 2HTPP at coverages below ~0.5 monolayer reacts with Mg²⁺ ions from corner, edge and step sites to form MgTPP, whereas at higher coverages, the porphyrin remains in its free-base form due to the lower mobility of the molecules at higher coverage and blocking of the active sites.

The next step was to investigate an already metalated porphyrin on MgO thin films [P4]. CoTPP was chosen because it has been shown to be a promising catalyst when bound to a surface, for instance for the reduction of nitric oxide and the oxidation of organic alcohols.^{10,60} Figure 20 shows a room temperature coverage series of CoTPP on an MgO film, followed by synchrotron radiation XPS at the endstation I09 at Diamond Lightsource, UK. The Co 2p_{3/2} multilayer signal²¹ exhibits the typical multiplet shape due to reasons discussed in Chapter 2.1.2. A significant difference between multilayer and submonolayer films is an additional contribution in the submonolayer range which is shifted by -2.2 eV with respect to the main signal. This indicates that a fraction of molecules (~1/5) in the first CoTPP layer is able to interact electronically with the surface, but the majority (~4/5) does not, since the largest fraction of the signal is similar to that found in the multilayer. This finding is supported by the N 1s spectra, which show significantly larger peak widths in the submonolayer region as well as an asymmetry towards the higher binding energy side of the spectrum.

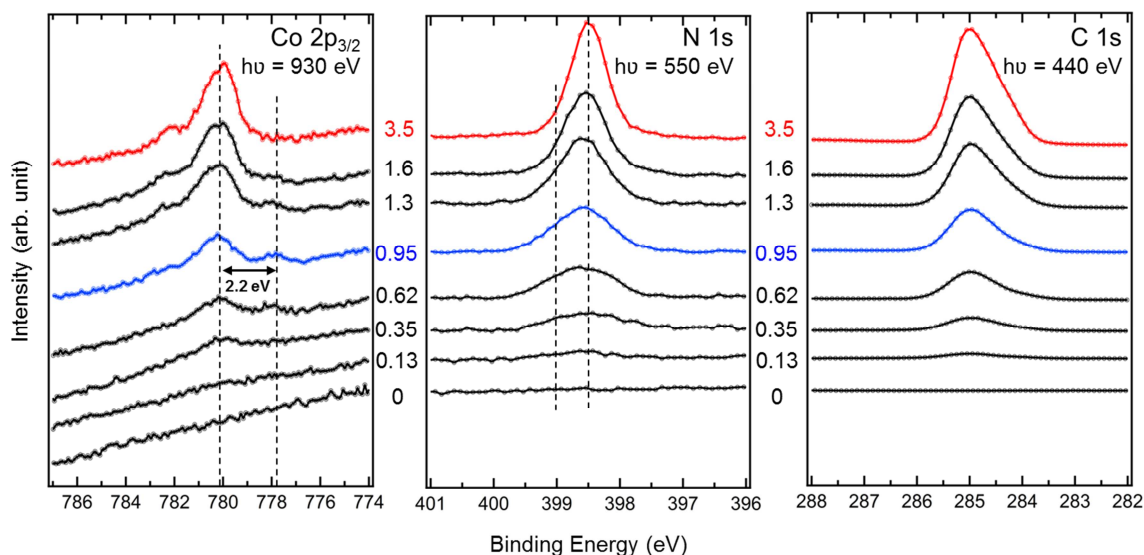


Figure 20. Coverage series of CoTPP on MgO(100). Coverages are indicated next to the columns in the unit monolayer. The red spectrum corresponds to multilayers, the blue to an almost completed monolayer.

Similar two-peak structures for metal centers were found for CoTPP and other tetrapyrroles adsorbed on Au(111).^{22,61} The authors explained this phenomenon by a lateral variation of surface electronic structure, due to the herringbone reconstruction of Au(111). On MgO, a similar explanation is possible. The MgO valence band is dominated by O 2p contributions and is therefore located at the oxygen ions.⁶² It is plausible that only CoTPP molecules that adsorb with their Co(II) center on top of an oxygen ion can undergo an interaction with the valence band. Indeed, a CoTPP unit cell in which 1/5 of molecules are adsorbed with their metal center directly on top of an oxygen ion is possible and in agreement with previously found CoTPP unit cells on other substrates.^{63,64} A drawing of that unit cell can be found in [P4].

The signature of the interaction between the cobalt metal center and the MgO valence band is also visible in UPS. In the region close to the Fermi Edge (Figure 21 right chart), the multilayer CoTPP spectrum shows the HOMO of CoTPP as expected at 2.2 eV binding energy,²¹ the MgO reference spectrum displays no signal. The monolayer CoTPP/MgO spectrum shows an additional signal at 0.7 eV that has no counterpart in one of the other spectra and must consequently originate from the interaction between CoTPP and MgO. In agreement with the XPS data, only a fraction of molecules seem to contribute to that signal, since most of the intensity is still located at the CoTPP HOMO position at 2.2 eV.

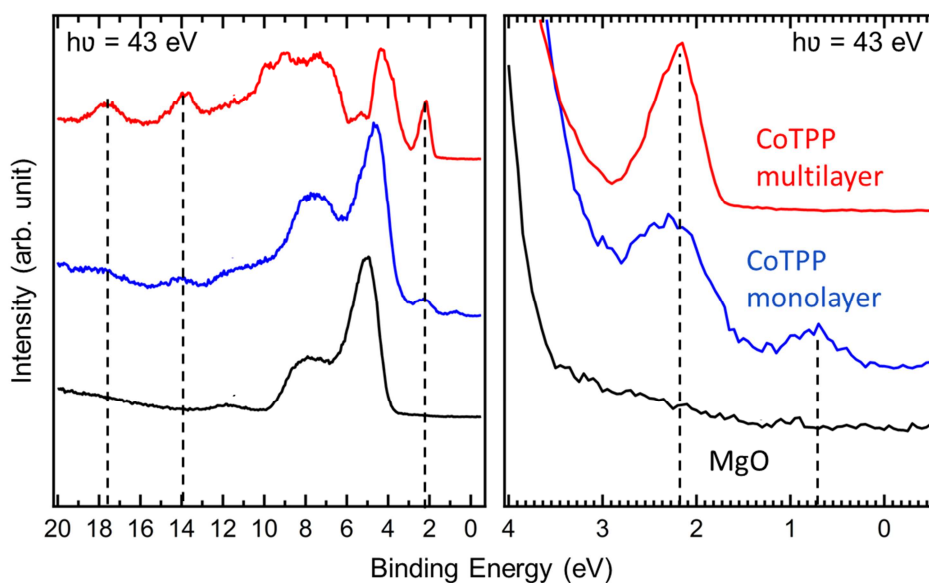


Figure 21. UP spectra of a) CoTPP multilayers, b) 0.9 monolayer CoTPP on a 10 monolayer MgO thin film and c) the pristine MgO thin film as a reference.

The next step was to investigate possible reactions of CoTPP at elevated temperatures. Figure 22 shows the evolution of XP spectra as a sample with CoTPP multilayers (3.5 monolayers) on MgO are heated to 550 K for 2 minutes. The carbon intensity drops to 0.35 monolayers, indicative of molecule desorption. The carbon to nitrogen ratio stays constant during heating, which points to still intact porphyrin molecules. This is a significant difference compared to the common behavior on metal surfaces on which closed monolayers of porphyrins are yielded when heating to comparable temperatures. The fact that the resulting coverage on MgO is much lower could indicate weaker molecule-substrate interactions than on metal substrates. The remaining molecules remain on the surface up to at least 650 K (Figure shown in [P4]), presumably because they are interlinked covalently by intermolecular C-C bond formation, which is likely to occur at these temperatures on metal substrates.^{65,66,67} The signal in the Co $2p_{3/2}$ region disappears completely (Figure 22 b), while the N 1s signal still consists of a single peak which speaks for a metalated and not a free base porphyrin. The N 1s binding energy position is consistent with MgTPP, as the reference measurement (Figure 22d) shows. Since we have seen before that free-base porphyrins can be metalated with Mg^{2+} ions from MgO ([P3]), it is tantalising to propose a metal center exchange between Co(II) and Mg(II), especially when considering the very similar radii of the two ions⁶⁸ and the fact that a metal center exchange on a surface in vacuum has already been conducted by Doyle et al., who exchanged nickel metal centers of NiTPP with copper.³³ Recently conducted temperature-programmed desorption measurements (not shown) confirmed the formation of MgTPP, but unfortunately also the presence of 10 % 2HTPP impurities in CoTPP. Thus, we believe the formation of MgTPP to be predominantly the result of self-metalation of 2HTPP and not ion exchange of CoTPP.

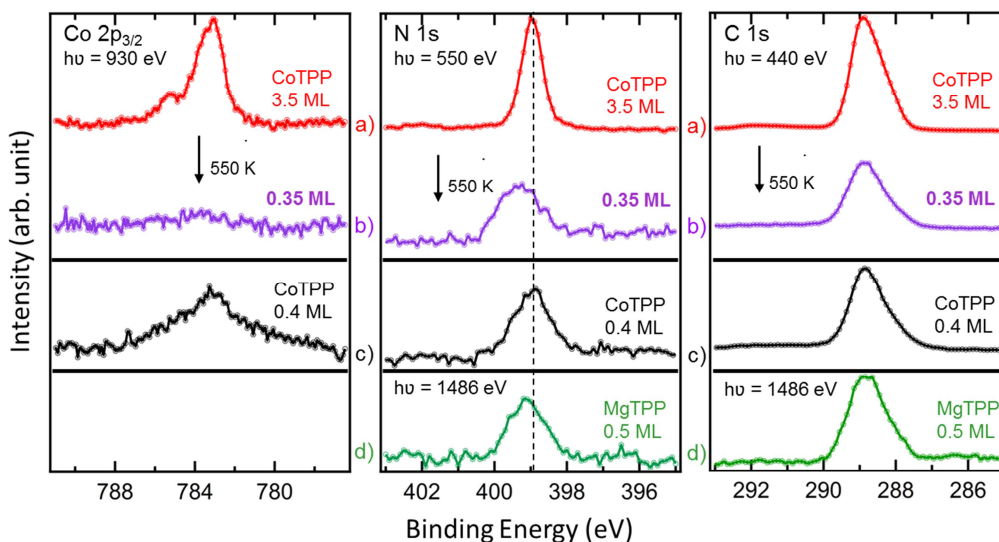


Figure 22. XP spectra of MgO with a) multilayer CoTPP, b) the same multilayer heated to 550 K for 2 minutes, c) 0.4 monolayer CoTPP and d) 0.5 monolayer MgTPP, indicating the possible formation of MgTPP.

4.3 Anhydride formation on a silver surface

In order to develop functional devices based on organic/oxide interfaces, it is important to learn about different ways to attach molecules to surfaces. One option is use one or more functional linker groups, e.g. carboxylic acids or phosphonates that can form a covalent link to the surface. As a model system for a carboxylic acid functionalized porphyrin, we used phthalic acid (structural model depicted in Figure 23). Besides from depositing it on MgO, we also did experiments on pure Ag(100). The results turned out to be interesting and are presented in this chapter.

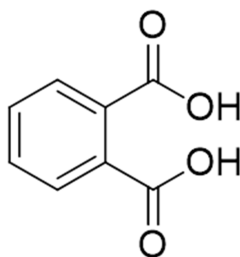


Figure 23. Structural model of phthalic acid.

Figure 24 depicts low-temperature XP O 1s and C 1s spectra obtained at the Material Science Beamline at Synchrotron Trieste, Italy. They show 0.5 monolayer of phthalic acid deposited on Ag(100) and heated stepwise to the indicated temperatures for 2 min each. In the top chart, an Al K_{α} multilayer spectrum is shown a reference. A comparison between the multilayer spectrum and the 110 K spectrum of 0.5 monolayer shows that they are almost identical, which confirms that molecules are intact at 110 K. The O 1s spectrum can be described by two components with a 2:2 ratio, hydroxyl oxygen at 533.6 eV and carbonyl oxygen at 532.5 eV, in agreement with previous XPS studies on carboxylic acids.^{69,70} The C 1s spectra show two peaks at 285.4 and 289.7 eV, which are assigned to

the benzene carbon atoms and carboxylic carbon atoms, respectively, with the expected intensity ratio of 6:2. Upon heating, three stable reaction plateaus can be observed: 150-200 K, 250-300 K and 400-450 K. The first plateau (150-200 K) is characterized by asymmetric peak shapes, indicating multiple species. We will therefore start with the discussion of the second plateau (250-300 K). The O 1s signal can be described by two components in a 1:2 ratio and the ratio of oxygen to carboxylic carbon has changed from 4:2 (fixed ratio for phthalic acid) to 3:2.2, indicating that the surface species at 250–300 K has one oxygen atom per molecule less than the species at 110 K.

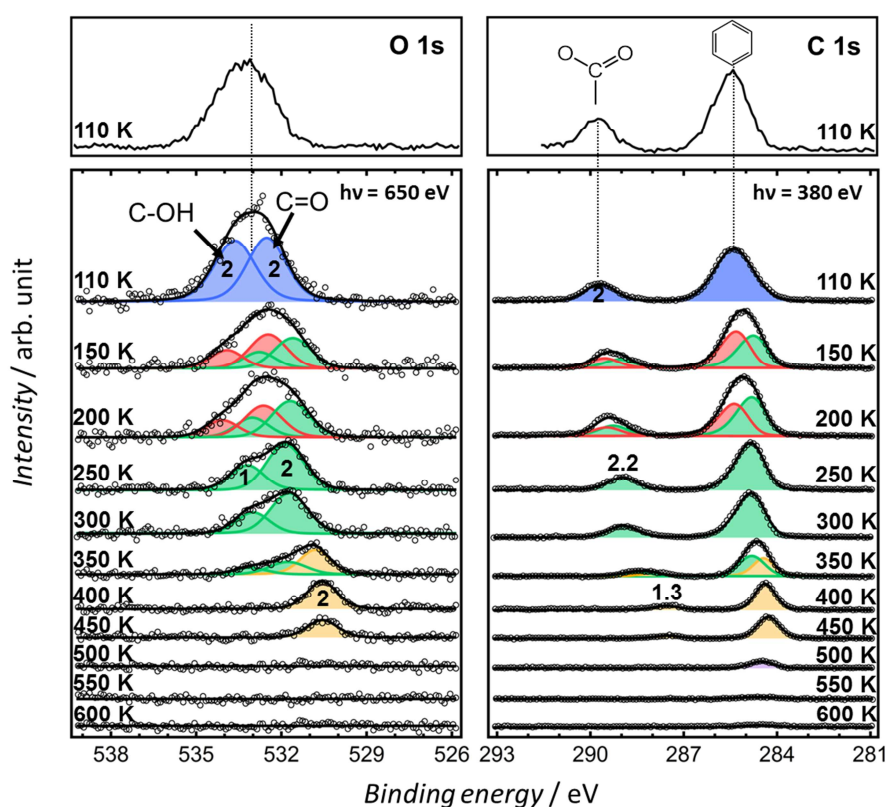


Figure 24. O 1s and C 1s Sychrotron Radiation-XP spectra of 0.5 ML phthalic acid deposited on Ag(100) at 110 K and heated, stepwise, to 600 K. On the top, Al K α multilayer spectra of phthalic acid on Ag(100) are depicted as a reference.

Phthalic acid is known to react when heated to form anhydrides, and both of the above observations agree with anhydride formation. If anhydride is formed, water should be released. Indeed, TPD measurements conducted in our home lab in Erlangen show the evolution of water ($m/z = 18$) as depicted in Figure 25. The main desorption features for phthalic acid are a peak at 150 K and a shoulder at 170 K. The latter increases with coverage and develops into the dominating peak at ~ 4 monolayers, while the 150 K peak is coverage-independent and also present if phthalic anhydride is initially deposited on the surface. We therefore assign the 150 K feature to residual gas water in the

vacuum chamber which adsorbs on the sample at low temperature and the 170 K peak to water formation as a consequence of anhydride formation.

If phthalic anhydride is formed, it might desorb at higher temperatures and give rise to a TPD signal. Figure 26 shows TPD spectra of all species between $m/z = 1$ and $m/z = 300$ that could be detected by our mass spectrometer while heating the sample to 700 K: 18 (water), 44 (CO_2), 78 (benzene), and 104 (phthalic anhydride) after deposition of 0.5 ML phthalic acid (black) and 0.5 ML phthalic anhydride (blue) on Ag(100).

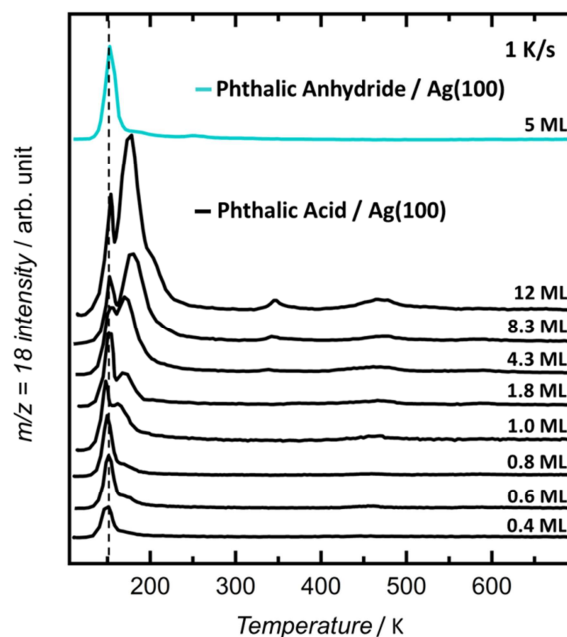


Figure 25. TPD spectra of water ($m/z = 18$) from phthalic acid deposited on Ag(100) at 110 K at a heating rate of 1 K/s. The topmost spectrum shows the corresponding spectrum of initially deposited phthalic anhydride instead of phthalic acid.

Mass 104 was chosen for phthalic anhydride because it was the most intense fragment. The spectra after deposition of phthalic acid show desorption of phthalic anhydride, supporting the idea of anhydride formation. The 300 K desorption peak is almost identical with the observed peak after direct deposition of phthalic anhydride and thus we assign it to adsorbed phthalic anhydride produced by phthalic acid on the surface. However, the 450 K peak is absent for the phthalic anhydride covered surface, it must therefore be the decomposition product of another species.

At this point, it is important to state that the temperatures from the TPD and XPS measurements cannot be compared directly. The XPS spectra were measured at 110 K after heating the sample to the indicated temperatures for 2 minutes each, while the temperature was ramped at a rate of 1 K/s for the TPD measurements. Furthermore, at the endstation of the Material Science Beamline, where the XPS data was collected, the sample temperature was measured with thick thermocouples in contact with the backside of the crystal which does not allow for an optimal contact. Therefore, the indicated

temperatures are lower than the actual temperatures. For direct comparison, we performed additional TPD measurements where the heating was stopped at 330 K and 495 K (green and orange vertical lines in Figure 26), cooled back down and measured the O 1s XP spectra that are displayed in the insets in Figure 26. A comparison with Figure 24 shows that the spectrum after heating to 330 K corresponds to the second plateau in Figure 24 (250-300 K) and the one after heating to 495 K to the third plateau (400-450 K).

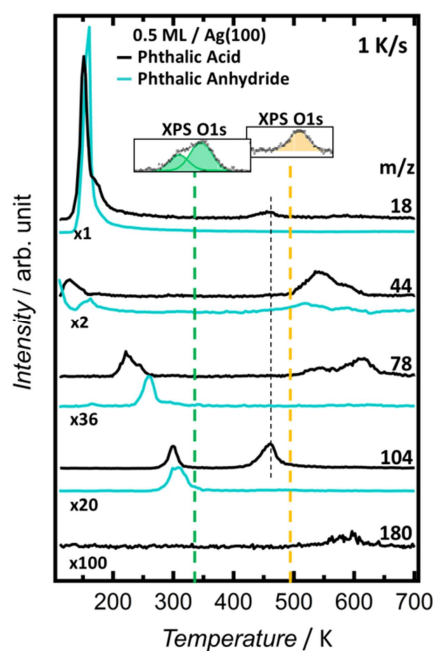


Figure 26. TPD spectra of water ($m/z = 18$), CO_2 ($m/z = 44$), benzene ($m/z = 78$) and phthalic anhydride (fragment with $m/z = 104$) from 0.5 ML phthalic acid (black lines) and 0.5 ML phthalic anhydride (blue lines) on Ag(100) at 1 K/s. $m/z = 180$ is an unknown component with very low intensity.

Since phthalic anhydride already desorbs at 300 K in the TPD spectrum, the species characterized by the inset in Figure 26 after heating to 330 K cannot be phthalic anhydride. Nevertheless, the 2:1 ratio in the O 1s region and the oxygen to carbon ratio determined by XPS points towards an anhydride.

The puzzle can be solved as follows: it is reasonable to assume that the phthalic acid molecules form hydrogen bonded networks on the surface at low temperature which leads to a close vicinity of adjacent molecules. Thus, we propose that anhydride formation does not only occur between two acid groups in one molecule, but also between groups of adjacent molecules which leads to the formation of dimeric- and/or polymeric anhydrides. Polyanhydrides are water-soluble polymers that are used, for example, for drug delivery within the body.⁷¹ In XPS, polyanhydrides would show the same signature as monomers,⁷² but would not desorb, instead decompose at higher temperatures. We therefore believe that the observed anhydride formation between 110 and 150 K produces both monomeric and polymeric anhydrides (see Figure 27). The former desorb at 300 K

(TPD) while the latter remain on the surface and are observed in the second plateau in Figure 24. Consequently, the first plateau in Figure 24 corresponds to a mixture of phthalic anhydride and polyanhydrides, we fitted the O 1s and C 1s spectra therefore with two components of the same splitting and the same width (exact numbers in [P5]).

In Figure 26, two additional features are visible below room temperature, which we attribute to contamination. CO₂ (44) degasses from the Mo-heating wires and the benzene peak (78) is close to the desorption peak of pure benzene from Ag(111).⁷³ It is likely that it originated from benzene coadsorption from the residual gas, presumably originating from the phthalic acid/ anhydride evaporator.

The third plateau in Figure 24 is observed from 400-450 K and corresponds to temperatures above 495 K in TPD. The O 1s signal consists of a single, narrow peak consistent with a single oxygen species. The binding energy shift speaks for a carboxylate species (COO⁻)^{69,74} which would explain the measured oxygen- to carboxylic carbon ratio of 2:1.3 that is close to the expected 2:1 for a carboxylate. This is also in agreement with a previous study on Cu(110), where phthalic anhydride was found to form carboxylates upon heating.⁷⁵ The carboxylic carbon to aromatic carbon ratio of 1:6.3 indicates one carboxylic acid group per benzene ring. The loss of carbon is reflected in the TPD spectrum (Figure 26) as desorption of phthalic anhydride at 450 K. The carboxylate could be upright standing, as previously observed for different carboxylates on copper,^{76,77} or flat-lying with adatoms linking adjacent carboxylate groups together, as observed for other systems.^{70,76}

Upon heating above 450 K, first oxygen and then carbon disappears from the surface (Figure 24). This observation is in line with the TPD measurements which show desorption of CO₂ and benzene above 500 K. As the amount of carbon remaining on the surface is much lower than expected considering the hydrogen balance of the mentioned reactions, we suggest that the missing carbon is lost by diffusion into the bulk of the Ag(100) crystal. All reactions are summarized in Figure 27.

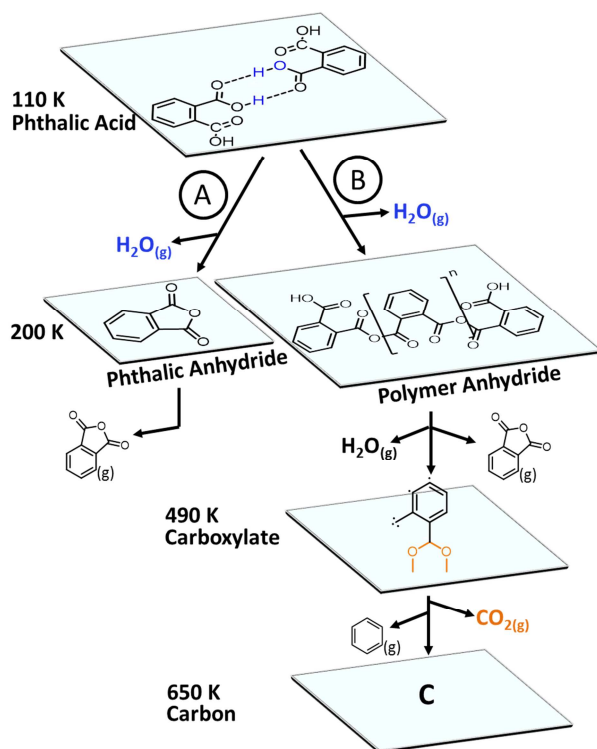


Figure 27. Proposed reaction scheme for the temperature-dependent reactions of phthalic acid on Ag(100).

5 Conclusion

In the present thesis, porphyrin reactions at solid/liquid interfaces and on magnesium oxide surfaces were investigated with X-ray photoelectron spectroscopy (XPS) and ultra-violet photoelectron spectroscopy (UPS). The temperature-dependent reactions of phthalic acid on Ag(100) were investigated using a combination of XPS and temperature-programmed desorption (TPD).

The main purpose of the experiments at **solid/liquid interfaces** was to find out if porphyrins adsorbed on a surface react the same way as porphyrins do in homogeneous solution. To target this issue, three test reactions that have been studied extensively in liquid phase were performed by exposing surface porphyrins on a Au(111) single crystal to aqueous solutions:

- 1) Metalation of 2HTPP free-base porphyrins with dissolved zinc ions,
- 2) Exchange of the Zn(II) metal center of ZnTPP with Cu(II)
- 3) Demetalation of ZnTPP in acidic solution.

It was found that metalation and metal center exchange happen spontaneously at room temperature just as they would happen in liquid phase. However, we did not observe any demetalation, even though the pH values of our solutions were acidic enough to have demetalated the porphyrin instantaneously in homogeneous solution. We explain that finding by a stabilization of the reaction intermediate through surface coordination of the outgoing ion.

Upon **adsorption on MgO**, it was found that low coverages of 2HTPP react at room temperature with Mg^{2+} -ions from step, corner and edge sites to form MgTPP and hydroxyl groups. This represents a new finding, because porphyrin metalation by substrate atoms was previously only reported on metal surfaces, where a surface atom is oxidized and incorporated into the porphyrin macrocycle. On MgO, the reaction has to proceed as an ion exchange, similar as it does in homogeneous solution.

Already metalated porphyrins, CoTPP, adsorb in two different modes on MgO surfaces. A fraction shows a strong electronic interaction, presumably adsorbing on-top of oxygen ions, while the majority shows no electronic interaction with the surface. When the sample is heated to 550 K, most molecules desorb, indicating a weaker molecule-surface bond than on most metal surfaces, where a closed monolayer remains at these temperatures.

Furthermore, the temperature-dependent reactions of **phthalic acid on Ag(100)** were followed using a combination of temperature programmed desorption (TPD) measurements and high-resolution XPS. It was found that intermolecular as well as intramolecular anhydride formation takes place. The monomeric anhydride desorbs at 300 K, while the polymer remains on the surface and reacts at 490 K

to form a carboxylate. The carboxylate decomposes into benzene and CO_2 , leaving only little carbon on the surface at 650 K.

6 Outlook

Further experiments on the solid/liquid interface could include other surfaces than Au(111) to investigate whether the surface has an influence on the porphyrin reactivity towards metalation, demetalation and ion exchange. Another interesting experiment would be to attempt demetalation with upright standing porphyrin molecules that should not be able to form a stabilized intermediate by surface coordination because their central cavity is too far away from the surface.

Concerning experiments on oxide surfaces, researchers should move on towards anchoring porphyrins covalently. Different types of linker groups should be investigated in order to achieve a high level of control over molecule-substrate interactions and thereby molecule orientation, site-specific adsorption, thermal stability etc. Furthermore, the research should be extended to different oxide surfaces with high potential for applications such as TiO_2 and CoO .

7 Zusammenfassung

Im Rahmen der vorliegenden Arbeit wurden die Reaktionen von Porphyrinen an flüssig/festen Grenzflächen und auf Magnesiumoxid-Oberflächen sowie von Phthalsäure auf Ag(100) mit Hilfe von Röntgen-Photoelektronenspektroskopie (XPS), Ultraviolet-Photoelektronenspektroskopie (UPS) und Temperatur-programmierter Desorption (TPD) untersucht.

Das Hauptziel der Experimente an **flüssig/festen Grenzflächen** war herauszufinden, ob an festen Oberflächen adsorbierte Porphyrine die gleiche Reaktivität wie Porphyrine in homogener Lösung aufweisen. Um das zu überprüfen wurden drei Testreaktionen, welche zuvor bereits ausführlich in flüssiger Phase studiert worden, herausgegriffen und mit adsorbierten Porphyrinen auf einem Au(111)-Einkristall durchgeführt:

- 1) Metallierung von 2HTPP freie-base Porphyrinen mit gelösten Zinkionen
- 2) Austausch des Zn(II) Metallzentrums in ZnTPP durch Cu(II)
- 3) Demetallierung von ZnTPP in saurer Lösung

Es stellte sich heraus, dass Metallierung und Metallzentrenaustausch bei Raumtemperatur ebenso stattfinden wie in homogener Lösung, es konnte aber keine Demetallierung in saurer Lösung nachgewiesen werden. Obwohl die verwendeten pH-Werte so niedrig waren, dass in homogener Lösung sofort eine Demetallierung stattgefunden hätte, blieb das Zn(II) Metallzentrum an das Porphyrin koordiniert. Eine mögliche Erklärung ist, dass das austretende Ion an die Oberfläche koordiniert und das Reaktionsintermediat dadurch stark gegenüber dem Produkt stabilisiert wird.

Beim **Abscheiden auf Magnesiumoxid** stellte sich heraus, dass 2HTPP bei niedrigen Bedeckungen mit Mg^{2+} -Ionen an Stufen, Ecken und Kanten unter der Bildung von MgTPP und Hydroxylgruppen reagiert. Das ist insofern eine neue Erkenntnis, als dass Porphyrin Metallierung durch Substratome bisher nur auf Metalloberflächen beobachtet wurde, wobei ein Metallatom oxidiert und vom Porphyrin Makrozyklus aufgenommen wird. Auf Magnesiumoxid muss die Reaktion hingegen als ein Ionenaustausch ablaufen, ähnlich wie es in homogener Lösung der Fall ist.

Metalloporphyrine, CoTPP, adsorbieren in zwei unterschiedlichen Adsorptionsmodi auf MgO. Ein Teil der Moleküle weist eine starke elektronische Wechselwirkung mit der Oberfläche auf, möglicherweise durch eine Adsorption des Metallzentrums direkt auf einem Sauerstoffanion des Oxids. Der größte Teil der Moleküle zeigt jedoch keine elektronische Wechselwirkung mit dem Substrat. Beim Heizen der Probe auf 550 K desorbieren fast alle Moleküle, was auf eine schwächere Molekül-Substrat Wechselwirkung hinweist als dies bei Metalloberflächen der Fall ist. Bei letzteren bleibt beim Heizen auf vergleichbare Temperaturen eine geschlossene Monolage zurück.

Zusätzlich wurden die temperaturabhängigen Reaktionen von **Phthalsäure auf Ag(100)** mit einer Kombination aus TPD und hochauflösender XPS entschlüsselt. Es stellte sich heraus, dass sowohl intra- als auch intermolekulare Anhydridbildung stattfindet. Das monomerische Anhydrid desorbiert bei 300 K, während das polymerische auf der Oberfläche zurück bleibt und bei 490 K unter Bildung eines Carboxylates reagiert. Das Carboxylat zersetzt sich unter Bildung von Benzol und Kohlendioxid, während ein kleiner Teil des Kohlenstoffs auf der Oberfläche zurück bleibt.

8 Acknowledgement

This thesis would not have been possible without the support of many people. I would like to thank:

Professor Hans-Peter Steinrück for providing an excellent scientific and social environment and letting me take part in it.

Dr. Ole Lytken for teaching- and guiding me through the world of science with endless patience.

Dr. Federico Williams, my supervisor from Buenos Aires, who showed me how to be passionate about science and helped me to not get lost in Argentina.

My colleagues who worked together with me in the lab, Daniel Wechsler, Michael Röckert, Quratulain Tariq, Liang Zhang, Florencia Marchini and Mariana Hamer as well as the people who shared the office with me, Michael Lepper, Florian Vollnhals, Martin Drost and Fan Tu.

All other people from the PC II chair for the friendly working atmosphere.

My collaboration partners from funCOS and the group of Prof. Norbert Jux.

The beamline staff from the Material Science Beamline at Elettra Synchrotron and from I09 Beamline at the Diamond Light Source for their excellent assistance.

The electrician Hans-Peter Bäumlner, the engineer Bernd Kress and the whole mechanical workshop team around Friedhold Wölfel for their great job in building, repairing and fixing all kinds of devices, machines and parts.

Finally, I want to thank my mother for her endless support and my whole family for believing in me. Thank you to Hanna, for bringing out the best in me.

9 List of References

- [1] Migrom, L. R., *The Colours of Life. An Introduction to the Chemistry of Porphyrins and Related Compounds. Oxford University Press* **1997**.
- [2] Fenton, D. E., *Biocoordination Chemistry, Oxford Science Publications: Oxford* **1995**.
- [3] da Silva, J. J.; Williams, R. J. P., *The Biological Chemistry of the Elements, Clarendon Press: Oxford* **1991**.
- [4] Lavalle, D. K., *Mol. Struct. Energ.* **1988**, *9*, 279.
- [5] Riedel, E.; Janiak, C.; Klapötke, T. M.; Meyer, H.-J., *Moderne Anorganische Chemie. Walter de Gruyter GmbH & Co. KG, Berlin* **2007**, 821.
- [6] Kadish, K. M.; Guillard, R., *Handbook of Porphyrin Science, Vol. 1-35. World Scientific Publishing Co. Singapore* **2010-2014**.
- [7] Campbell, W. M.; Jolley, K. W.; Wagner, P.; Wagner, K.; Walsh, P. J.; Gordon, K. C.; Schmidt-Mende, L.; Nazeeruddin, M. K.; Wang, Q.; Grätzel, M.; Officer, D. L., *Highly Efficient Porphyrin Sensitizers for Dye-Sensitized Solar Cells. J. Phys. Chem. C* **2007**, *111*, 11760-11762.
- [8] Grätzel, M., *Dye-sensitized solar cells. J. Photochem. Photobiol. C* **2003**, *4*, 145-153.
- [9] Rakow, N. A.; Suslick, K. S., *A colorimetric sensor array for odour visualization. Nature* **2000**, *406*, 710-713.
- [10] Mochida, I., *A kinetic study on reduction of nitric oxide over cobalt tetraphenylporphyrin supported on titanium dioxide. J. Catal.* **1982**, *77*, 519-526.
- [11] Gottfried, J. M., *Surface chemistry of porphyrins and phthalocyanines. Surf. Sci. Rep.* **2015**, *70*, 259-379.
- [12] Auwärter, W.; Eciija, D.; Klappenberger, F.; Barth, J. V., *Porphyrins at interfaces. Nat. Chem.* **2015**, *7*, 105-20.
- [13] Marbach, H.; Steinrück, H. P., *Studying the dynamic behaviour of porphyrins as prototype functional molecules by scanning tunnelling microscopy close to room temperature. Chem. Commun.* **2014**, *50*, 9034-9048.
- [14] Barth, J. V., *Fresh perspectives for surface coordination chemistry. Surf. Sci.* **2009**, *603*, 1533-1541.
- [15] Rojas, G.; Chen, X.; Bravo, C.; Kim, J.-H.; Kim, J.-S.; Xiao, J.; Dowben, P. A.; Gao, Y.; Zeng, X. C.; Choe, W.; Enders, A., *Self-assembly and properties of nonmetalated tetraphenylporphyrin on metal substrates. J. Phys. Chem. C* **2010**, *114*, 9408-9415.
- [16] Buchner, F.; Xiao, J.; Zillner, E.; Chen, M.; Röckert, M.; Ditze, S.; Stark, M.; Steinrück, H.-P.; Gottfried, J. M.; Marbach, H., *Diffusion, rotation, and surface chemical bond of individual 2H-tetraphenylporphyrin molecules on Cu(111). J. Phys. Chem. C* **2011**, *115*, 24172-24177.

- [17] Buchner, F.; Zillner, E.; Rockert, M.; Glassel, S.; Steinrück, H. P.; Marbach, H., Substrate-mediated phase separation of two porphyrin derivatives on Cu(111). *Chem. Eur. J.* **2011**, *17*, 10226-10229.
- [18] Buchner, F.; Flechtner, K.; Bai, Y.; Zillner, E.; Kellner, I.; Steinrück, H.-P.; Marbach, H.; Gottfried, J. M., Coordination of iron atoms by tetraphenylporphyrin monolayers and multilayers on Ag(111) and formation of iron-tetraphenylporphyrin. *J. Phys. Chem. C* **2008**, *112*, 15458-15465.
- [19] Chen, M.; Feng, X.; Zhang, L.; Ju, H.; Xu, Q.; Zhu, J.; Gottfried, J. M.; Ibrahim, K.; Qian, H.; Wang, J., Direct synthesis of nickel(II) tetraphenylporphyrin and its interaction with a Au(111) surface: a comprehensive study. *J. Phys. Chem. C* **2010**, *114*, 9908-9916.
- [20] Franke, M.; Marchini, F.; Steinruck, H. P.; Lytken, O.; Williams, F. J., Surface porphyrins metalate with Zn ions from solution. *J. Phys. Chem. Lett.* **2015**, *6*, 4845-4849.
- [21] Lukasczyk, T.; Flechtner, K.; Merte, L. R.; Jux, N.; Maier, F.; Gottfried, J. M.; Steinrück, H. P., Interaction of cobalt(II) tetraarylporphyrins with a Ag(111) surface studied with photoelectron spectroscopy. *J. Phys. Chem. C* **2007**, *111*, 3090-3098.
- [22] Schmid, M.; Zirzmeier, J.; Steinrück, H. P.; Gottfried, J. M., Interfacial interactions of iron(II) tetrapyrrole complexes on Au(111). *J. Phys. Chem. C* **2011**, *115*, 17028-17035.
- [23] Wang, C.; Fan, Q.; Hu, S.; Ju, H.; Feng, X.; Han, Y.; Pan, H.; Zhu, J.; Gottfried, J. M., Coordination reaction between tetraphenylporphyrin and nickel on a TiO₂(110) surface. *Chem. Commun.* **2014**, *50*, 8291-8294.
- [24] Lovat, G.; Forrer, D.; Abadia, M.; Dominguez, M.; Casarin, M.; Rogero, C.; Vittadini, A.; Floreano, L., Hydrogen capture by porphyrins at the TiO₂(110) surface. *Phys. Chem. Chem. Phys.* **2015**, *17*, 30119-30124.
- [25] Moors, M.; Krupski, A.; Degen, S.; Kralj, M.; Becker, C.; Wandelt, K., Scanning tunneling microscopy and spectroscopy investigations of copper phthalocyanine adsorbed on Al₂O₃/Ni₃Al(111). *Appl. Surf. Sci.* **2008**, *254*, 4251-4257.
- [26] Liu, L.; Zhang, W.; Guo, P.; Wang, K.; Wang, J.; Qian, H.; Kurash, I.; Wang, C. H.; Yang, Y. W.; Xu, F., A direct Fe-O coordination at the FePc/MoO(x) interface investigated by XPS and NEXAFS spectroscopies. *Phys. Chem. Chem. Phys.* **2015**, *17*, 3463-3469.
- [27] Hieringer, W.; Flechtner, K.; Kretschmann, A.; Seufert, K.; Auwärter, W.; Barth, J. V.; Görling, A.; Steinrück, H. P.; Gottfried, J. M., The surface trans effect: influence of axial ligands on the surface chemical bonds of adsorbed metalloporphyrins. *J. Am. Chem. Soc.* **2011**, *133*, 6206-22.
- [28] Cheung, S. K. D., F. L.; Fleischer, E. B.; Jeter, D. Y.; Krishnamurthy, M., Kinetic studies of the formation, acid-catalyzed solvolysis, and cupric ion displacement of a zinc porphyrin in aqueous solutions. *Bioinorg. Chem.* **1973**, *2*, 281-294.
- [29] Shamim, A.; Hambright, P., Exchange-reactions of transition-metal ions and labile cadmium porphyrins. *J. Inorg. Nucl. Chem.* **1980**, *42*, 1645-1647.
- [30] Baker, H.; Hambright, P.; Wagner, L.; Ross, L., Metal ion interactions with porphyrins. I. Exchange and substitution reactions. *Inorg. Chem.* **1973**, *12*, 2200-2202.

- [31] Hambricht, P.; Batinić-Haberle, I.; Spasojević, I., Meso tetrakis ortho-, meta-, and para-N-alkylpyridiniopor-phyrins: kinetics of copper(II) and zinc(II) incorporation and zinc porphyrin demetalation. *J. Porphyrins Phthalocyanines* **2003**, *7*, 139-146.
- [32] Grant, C.; Hambricht, P., Kinetics of electrophilic substitution reactions involving metal ions in metalloporphyrins. *J. Am. Chem. Soc.* **1969**, *91*, 4195-4198.
- [33] Doyle, C. M.; Cunniffe, J. P.; Krasnikov, S. A.; Preobrajenski, A. B.; Li, Z.; Sergeeva, N. N.; Senge, M. O.; Cafolla, A. A., Ni-Cu ion exchange observed for Ni(II)-porphyrins on Cu(111). *Chem. Commun.* **2014**, *50*, 3447-3449.
- [34] Marbach, H., Surface-mediated in situ metalation of porphyrins at the solid-vacuum interface. *Acc. Chem. Res.* **2015**, *48*, 2649-58.
- [35] Kretschmann, A.; Walz, M. M.; Flechtner, K.; Steinruck, H. P.; Gottfried, J. M., Tetraphenylporphyrin picks up zinc atoms from a silver surface. *Chem Commun (Camb)* **2007**, (6), 568-70.
- [36] Diller, K.; Klappenberger, F.; Marschall, M.; Hermann, K.; Nefedov, A.; Woll, C.; Barth, J. V., Self-metalation of 2H-tetraphenylporphyrin on Cu(111): an x-ray spectroscopy study. *J. Chem. Phys.* **2012**, *136*, 014705.
- [37] Einstein, A., Über einen die Erzeugung und Verwandlung des Lichtes betreffenden heuristischen Gesichtspunkt. *Ann. Physik* **1905**, *17*, 132-148.
- [38] Siegbahn, K., Electron Spectroscopy for Chemical Analysis (E.S.C.A), *Phil. Trans. R. Soc.* **1970**, *268*, 33-57.
- [39] Seah, M. P.; Dench, W. A., Quantitative electron spectroscopy of surfaces: a standard data base for electron inelastic mean free paths in solids. *Surf. Interface Anal.* **1979**, *1*, 2-11.
- [40] Nefedov, V. I., Multiplet structure of the $K_{\beta 1\beta}$ lines of transition elements *J. Struct. Chem.* **1964**, *5*, 649-651.
- [41] Gupta, R. P.; Sen, S. K., Calculation of multiplet structure of core p -vacancy levels II. *Phys. Rev. B* **1975**, *12*, 15-19.
- [42] Gupta, R. P.; Sen, S. K., Calculation of multiplet structure of core p -vacancy levels. *Phys. Rev. B* **1974**, *10*, 71-77.
- [43] Hüfner, S., Photoelectron Spectroscopy, Principles and Applications, *3. Auflage, Springer Berlin* **2003**.
- [44] Briggs, D.; Seah, M. P., Practical Surface Analysis Vol. 1: Auger and X-ray Photoelectron Spectroscopy, *Wiley Chichester* **1990**.
- [45] Röckert, M., Spectroscopic insights in the metalation and dehydrogenation of tetrapyrroles on well-defined metal substrates. *PhD thesis Erlangen* **2015**.
- [46] Chan, C. M.; Aris, R.; Weinberg, W. H., An analysis of thermal desorption mass spectra I. *Appl. Surf. Sci.* **1978**, *1*, 360-376.
- [47] de Jong, A. M.; Niemantsverdriet, J. W., Thermal desorption analysis: Comparative test of ten commonly applied procedures. *Surf. Sci.* **1990**, *233*, 355-365.

- [48] Falconer, J. L.; Schwarz, J. A., Temperature-programmed desorption and reaction: applications to supported catalysts. *Catal. Rev.* **2007**, *25*, 141-227.
- [49] Altieri, S.; Tjeng, L. H.; Sawatzky, G. A., Electronic structure and chemical reactivity of oxide-metal interfaces: MgO(100)/Ag(100). *Phys. Rev. B* **2000**, *61*, 16948-16955.
- [50] Jian-Wei, H.; Estrada, C. A.; Corneille, J. S.; Ming-Cheng, W.; Wayne Goodman, D., CO adsorption on ultrathin MgO films grown on a Mo(100) surface: an IRAS study. *Surf. Sci.* **1992**, *261*, 164-170.
- [51] Chakradhar, A.; Burghaus, U., Carbon dioxide adsorption on MgO(001)-CO₂ kinetics and dynamics. *Surf. Sci.* **2013**, *616*, 171-177.
- [52] Wollschläger, J.; Viernow, J.; Tegenkamp, C.; Erdös, D.; Schröder, K. M.; Pfnür, H., Stoichiometry and morphology of MgO films grown reactively on Ag(100). *Appl. Surf. Sci.* **1999**, *142*, 129-134.
- [53] Valeri, S.; Altieri, S.; del Pennino, U.; di Bona, A.; Luches, P.; Rota, A., Scanning tunnelling microscopy of MgO ultrathin films on Ag(001). *Phys. Rev. B* **2002**, *65*, 245410.
- [54] Schintke, S.; Messerli, S.; Pivetta, M.; Patthey, F.; Libioulle, L.; Stengel, M.; De Vita, A.; Schneider, W. D., Insulator at the ultrathin limit: MgO on Ag(001). *Phys. Rev. Lett.* **2001**, *87*, 276801.
- [55] Möller, F. A.; Magnussen, O. M.; Behm, R. J., In situ STM studies of Cu underpotential deposition on Au(100) in the presence of sulfate and chloride anions. *Phys. Rev. B* **1995**, *51*, 2484-2490.
- [56] De Luca, G.; Romeo, A.; Scolaro, L. M.; Ricciardi, G.; Rosa, A., Sitting-Atop metalloporphyrin complexes: experimental and theoretical investigations on such elusive species. *Inorg. Chem.* **2009**, *48*, 8493-507.
- [57] Fleischer, E. B.; Wang, J. H., The detection of a type of reaction intermediate in the combination of metal ions with porphyrins. *J. Am. Chem. Soc.* **1969**, *82*, 3498-3502.
- [58] Inada, Y.; Sugimoto, Y.; Nakano, Y.; Itoh, Y.; Funahashi, S., Formation and deprotonation kinetics of the sitting-atop complex of copper(II) ion with 5,10,15,20-tetraphenylporphyrin relevant to the porphyrin metalation mechanism. Structure of copper(II)-pyridine complexes in acetonitrile as determined by EXAFS spectroscopy. *Inorg. Chem.* **1998**, *37*, 5519-5526.
- [59] Smykalla, L.; Shukrynau, P.; Zahn, D. R. T.; Hietschold, M., Self-metalation of phthalocyanine molecules with silver surface atoms by adsorption on Ag(110). *J. Phys. Chem. C* **2015**, *119*, 17228-17234.
- [60] Berner, S.; Biela, S.; Ledung, G.; Gogoll, A.; Backvall, J.; Puglia, C.; Oscarsson, S., Activity boost of a biomimetic oxidation catalyst by immobilization onto a gold surface. *J. Catal.* **2006**, *244*, 86-91.
- [61] Bai, Y.; Sekita, M.; Schmid, M.; Bischof, T.; Steinrück, H. P.; Gottfried, J. M., Interfacial coordination interactions studied on cobalt octaethylporphyrin and cobalt tetraphenylporphyrin monolayers on Au(111). *Phys. Chem. Chem. Phys.* **2010**, *12*, 4336-44.
- [62] King, P. D. C.; Veal, T. D.; Schleife, A.; Zúñiga-Pérez, J.; Martel, B.; Jefferson, P. H.; Fuchs, F.; Muñoz-Sanjósé, V.; Bechstedt, F.; McConville, C. F., Valence-band electronic structure of

- CdO, ZnO, and MgO from x-ray photoemission spectroscopy and quasi-particle-corrected density-functional theory calculations. *Phys. Rev. B* **2009**, *79*, 205205.
- [63] Barlow, D. E.; Scudiero, L.; Hipps, K. W., Scanning tunneling microscopy study of the structure and orbital-mediated tunneling spectra of cobalt(II) phthalocyanine and cobalt(II) tetraphenylporphyrin on Au(111): Mixed Composition Films. *Langmuir* **2004**, *20*, 4413-4421.
- [64] Scudiero, L.; Barlow, D. E.; Mazur, U.; Hipps, K. W., Scanning tunneling microscopy, orbital-mediated tunneling spectroscopy, and ultraviolet photoelectron spectroscopy of metal(II) tetraphenylporphyrins deposited from vapor. *J. Am. Chem. Soc.* **2001**, *123*, 4073-4080.
- [65] In't Veld, M.; Iavicoli, P.; Haq, S.; Amabilino, D. B.; Raval, R., Unique intermolecular reaction of simple porphyrins at a metal surface gives covalent nanostructures. *Chem. Commun.* **2008**, *13*, 1536-1538.
- [66] Sun, Q.; Zhang, C.; Cai, L.; Xie, L.; Tan, Q.; Xu, W., On-surface formation of two-dimensional polymer via direct C-H activation of metal phthalocyanine. *Chem. Commun.* **2015**, *51*, 2836-2839.
- [67] Wiengarten, A.; Seufert, K.; Auwärter, W.; Eciija, D.; Diller, K.; Allegretti, F.; Bischoff, F.; Fischer, S.; Duncan, D. A.; Papageorgiou, A. C.; Klappenberger, F.; Acres, R. G.; Ngo, T. H.; Barth, J. V., Surface-assisted dehydrogenative homocoupling of porphine molecules. *J. Am. Chem. Soc.* **2014**, *136*, 9346-9354.
- [68] Shannon, R. D., Revised effective ionic radii and systematic studies of interatomic distances in halides and chalcogenides. *Acta Cryst.* **1976**, *32*, 751-767.
- [69] Lin, N.; Payer, D.; Dmitriev, A.; Strunskus, T.; Woll, C.; Barth, J. V.; Kern, K., Two-dimensional adatom gas bestowing dynamic heterogeneity on surfaces. *Angew. Chem. Int. Ed.* **2005**, *44*, 1488-1491
- [70] Stepanow, S.; Strunskus, T.; Lingenfelder, M.; Dmitriev, A.; Spillmann, H.; Lin, N.; Barth, J. V.; Wöll, C.; Kern, K., Deprotonation-driven phase transformations in terephthalic acid self-assembly on Cu(100). *J. Phys. Chem. B* **2004**, *108*, 19392-19397.
- [71] Kumar, N.; Langer, R. S.; Domb, A. J., Polyanhydrides: an overview. *Adv. Drug Deliv. Rev.* **2002**, *54*, 889-910.
- [72] Davies, M. C.; Khan, M. A.; Domb, A.; Langer, R.; Watts, J. F.; Paul, A. J., The analysis of the surface chemical-structure of biomedical aliphatic polyanhydrides using XPS and ToF-Sims. *J. Appl. Polym. Sci.* **1991**, *42*, 1597-1605.
- [73] Rockey, T. J.; Yang, M. C.; Dai, H. L., Adsorption energies, inter-adsorbate interactions, and the two binding sites within monolayer benzene on Ag(111). *J. Phys. Chem. B* **2006**, *110*, 19973-19978.
- [74] Fuhr, J. D.; Carrera, A.; Murillo-Quirós, N.; Cristina, L. J.; Cossaro, A.; Verdini, A.; Floreano, L.; Gayone, J. E.; Ascolani, H., Interplay between hydrogen bonding and molecule-substrate interactions in the case of terephthalic acid molecules on Cu(001) surfaces. *J. Phys. Chem. C* **2013**, *117*, 1287-1296.
- [75] Haq, S.; Bainbridge, R. C.; Frederick, B. G.; Richardson, N. V., Anhydride ring chemistry at a metal surface. *J. Phys. Chem. B* **1998**, *102*, 8807-8815.

- [76] Perry, C. C.; Haq, S.; Frederick, B. G.; Richardson, N. V., Face specificity and the role of metal adatoms in molecular reorientation at surfaces. *Surf. Sci.* **1998**, *409*, 512-520.
- [77] Frederick, B. G.; Ashton, M. R.; Richardson, N. V.; Jones, T. S., Orientation and bonding of benzoic-Acid, phthalic-anhydride and pyromellitic dianhydride on Cu(110). *Surf. Sci.* **1993**, *292*, 33-46.

10 Appendix [P1]-[P5]

[P1] [Surface Porphyrins Metalate with Zn Ions from Solution](#)

Matthias Franke, Florencia Marchini, Hans-Peter Steinrück, Ole Lytken, Federico J. Williams
J. Phys. Chem. Lett. **2015**, 6, 4845–4849

[P2] [Zinc Porphyrin Metal-Center Exchange at the Solid-Liquid Interface](#)

Matthias Franke, Florencia Marchini, Norbert Jux, Hans-Peter Steinrück, Ole Lytken, Federico J. Williams
Chem. Eur. J. **2016**, 22, 8520 – 8524

[P3] [Porphyrimetalation at MgO Surfaces: A Spectroscopic and Quantum Mechanical Study on Complementary Model Systems](#)

Johannes Schneider, Matthias Franke, Martin Gurrath, Michael Röckert, Thomas Berger, Johannes Bernardi, Bernd Meyer, Hans-Peter Steinrück, Ole Lytken, Oliver Diwald
Chem. Eur. J. **2016**, 22, 1744 – 1749

[P4] **Interfacial Interactions between CoTPP Molecules and MgO Thin Films**

Matthias Franke, Daniel Wechsler, Quratulain Tariq, Michael Röckert, Liang Zhang, Pardeep Kumar Takur, Natalya Tsud, Sofia Bercha, Kevin Prince, Tien-Lin Lee, Hans-Peter Steinrück, Ole Lytken
Submitted to PCCP

[P5] [Temperature-Dependent Reactions of Phthalic Acid on Ag\(100\)](#)

Matthias Franke, Florencia Marchini, Liang Zhang, Quratulain Tariq, Nataliya Tsud, Mykhailo Vorokhta, Martin Vondráček, Kevin Prince, Michael Röckert, Federico José Williams, Hans-Peter Steinrück, Ole Lytken
J. Phys. Chem. C **2015**, 119, 23580–23585